2

T1045F

(NASA-CR-124367) SPACE SHUTTLE DAMPER SYSTEM FOR GROUND WIND LOAD TESTS Final Report, 17 Apr. 1972 - 16 Apr. 1973 (Applied Dynamics Research Corp.) 68 p HC $5.50 CSCL 22B G3/31

N73-30845

Unclas 17808

Final Report

Space Shuttle Damper System For Ground Wind Load Tests

Conteact NAS8-28613 April 16, 1973

G. D. Robinson
J. R. Holt
C. S. Chang

Approved by: C. S. Chang
C. S. Chang

68

FOREWORD

This Final Technical Report is prepared by Applied Dynamics Research Corporation in partial fulfillment of MSFC Contract NAS8-28613, "Space Shuttle Damper System for Ground Wind Loads Tests." The period of performance of this contract was from April 17, 1972 to April 16, 1973.

Technical monitors for MSFC were Messrs. Paul W. Howard and Gary W. Johnson, S&E-AERO-AUE.

SUMMARY

An active damper system which was originally developed for a 5.5% Saturn IB/Skylab Ground Winds Model was modified and used for similar purposes in a Space Shuttle model. A second damper system which was originally used in a 3% Saturn V/Dry Workshop model was also modified and made compatible with the Space Shuttle model to serve as a back-up system.

Included in this final report are descriptions of the modified damper systems and the associated control and instrumentation.

TABLE OF CONTENTS

LIST OF ILLUSTRATIONS

Section 1

INTRODUCTION

Aeroelastically scaled models are used by NASA in wind tunnel tests to predict ground wind-induced loads (GWL) for launch vehicles in the on-pad, prelaunch configuration. One of the critical dynamic characteristics of an aeroelastic model is damping. In order to cover the normal range of damping expected for the full-scale vehicle and to determine the effect of damping on the induced dynamic loads, model damping must be adjustable and known accurately for each test configuration. For the Space Shuttle GWL program, tests were to be conducted in NASA/LaRC's 16-foot Transonic Dynamics Tunnel (TDT) using 100% Freon. It was desirable to have the capability of adjusting model damping remotely so that the number of entries into the tunnel test section could be significantly reduced and the test program duration minimized.

Active damper systems using velocity feedback and electromagnetic force generation had been used successfully in the past in both the Saturn/Apollo and the Skylab GWL programs. The damper system previously developed by Applied Dynamics Research Corporation (ADRC) for the IB/Skylab model (Reference 1) was modified on this project and adapted for the Space Shuttle GWL model.* A new control system was developed for optimum utilization of the electromechanical and electronic devices left over from previous MSFC GWL test programs. Instrumentation for conditioning, monitoring and distribution of model response transducer signals were also assembled and incorporated with the damper control system into a single package.

---

*Developed by McDonnel Douglas Corporatic:, see Reference (2).

The Space Shuttle GWL test program was conducted during the period 10 October through 15 November 1972. In addition to providing damping to the test model during wind tunnel tests, the damper system was also used heavily to conduct dynamic and static calibration tests and to set up data recorders and on-line data reduction systems.

The damper system previously developed for the Saturn V/Dry Workshop (Reference 3) was also modified and made compatible with the Space Shuttle model. However, this system did not see service during the wind tunnel test program.

Section 2

SYSTEM OUTLINE

The basic principle of the active damper is fairly simple: the response velocity vector at a selected point on the model is measured by two mutually perpendicular sensors. The output signals of these transducers drive two electromagnetic force generators which are oriented in the same directions as the corresponding sensors. The resultant force vector will coincide with the instantaneous velocity of the model. The magnitude of the force is proportional to that of the velocity. If the feedback polarity is such that the force is 180° out of phase with respect to the velocity vector, linear viscous damp dampint is added to the model. The damping coefficient is adjusted by adjusting the velocity signal-to-force gain. The two-channel damper system is outlined in block diagram form in Figure 1.

The force generators were originally developed for the Saturn IB/Skylab program. A detailed discussion of the development philosophy and design considerations are given in Reference 1. Major modifications of these force generators for the Space Shuttle GWL program include (a) the redesign and replacement of the force coils to provide a higher force output with respect to the power amplifier operating conditions*, and (b) the modification of the damper-model interface.

Due to physical constraints and the structural dynamics of the force generators, different types of velocity sensing schemes were necessary for the two damper channels. For each channel, however, the relative velocity of the model with respect to the force generator is measured by a specially developed transducer which is mounted directly above the force generators.

---

*The increase in force coil performance was achieved at a reduction of allowable stroke from $\pm$ 0.85" to $\pm$ 0.35". The reduced stroke capability was sufficient for the Space Shuttle model which is significantly shorter than the Saturn IB/Skylab model.

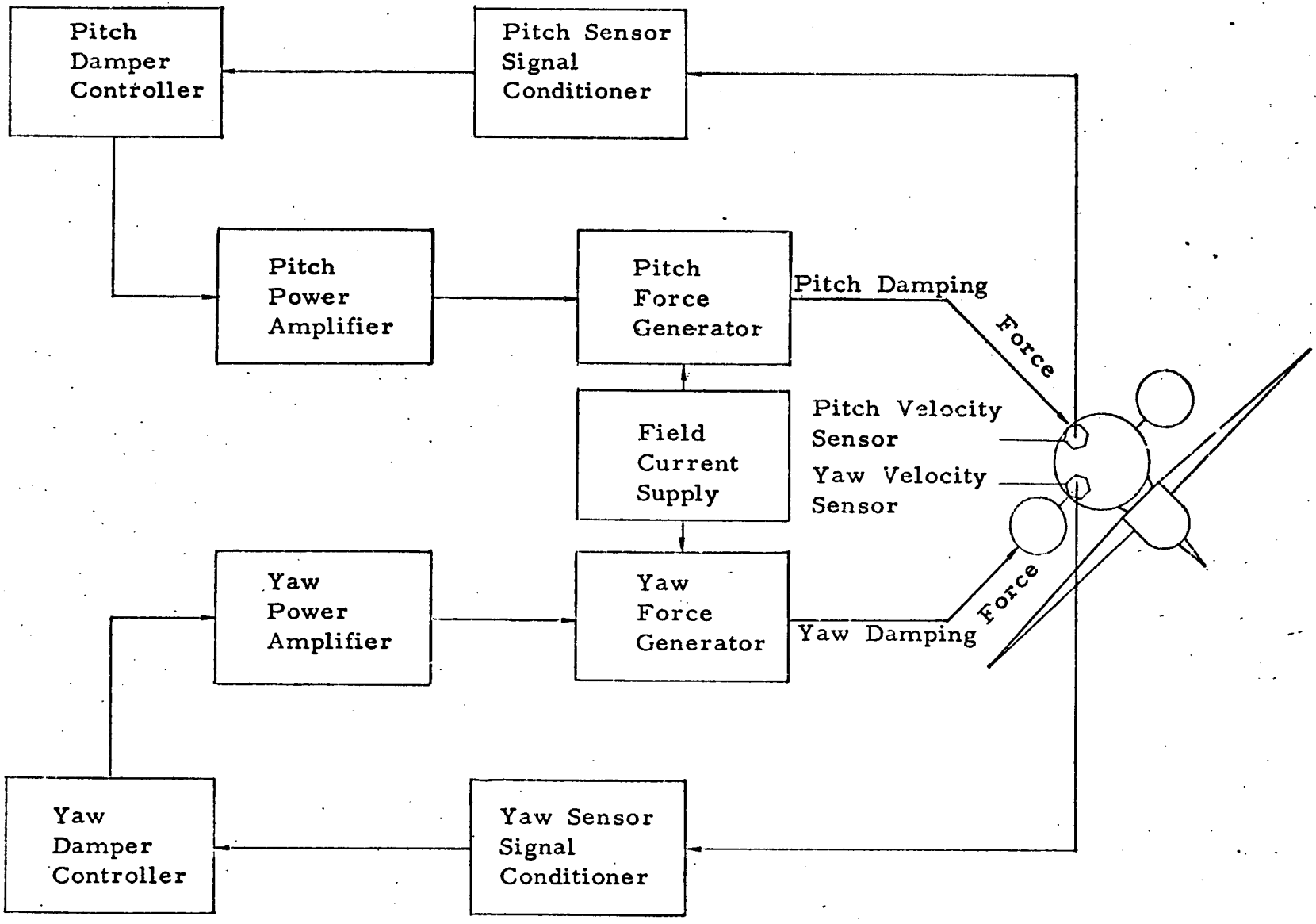

Fig 1 Damper System Block Diagram

Two separate and independent damper control units were developed for the two-directional damper system. These controllers also include means for conducting vibration checkout tests of the model, using the same power amplifiers and force generators which, during wind tunnel tests, functioned as dampers. Controllers are discussed in detail in Section 4.

Section 3

MECHANICAL MODIFICATIONS

3.1 Model-Damper Interface

Mechanically, the damper was designed for GWL tests of the Saturn IB/Skylab model. The Space Shuttle model, by comparison, is less than half as long and some 2" smaller in diameter. Mechanical modifications required to adapt the damper for the Space Shuttle application included the following:

(a) Four Mounting Brackets of the Damper Support Assembly were removed. These brackets are designated as Items No. 1, ADRC Dwg No. 20009-Revision B.*

(b) Four holes were drilled through the aluminum Ring of the Damper Support Assembly according to Note 5 of the above-mentioned (revised) drawing. The Ring itself was used as the interfacing member with the pace huttle model, using four 1-1/4" 1/4-28 machine screws through the above-mentioned holes. See ADRC Dwg. Nos. 20027 and 20009-Revision B.

3.2 Damper Support Assembly

For the shorter model, the curvature of the Upper and Lower Bearing Plates was increased from a 90" radius to a 50" radius according to Note 6, ADRC Dwg. No. 20010-Revision B and Note 10, ADRC Dwg. No. 20013-Revision B.

3.3 Force Coils

For the shorter model, the required stroke capability of the damper is significantly reduced. One additional inch of dimension thus became available for the force coil in all directions. New coils and coil carrying plates were designed and fabricated to take advantage of this available space. The same coil elements were used. They are:

---

* A complete set of drawings for the damper system are enclosed under separate covers as Appendix C of this report.

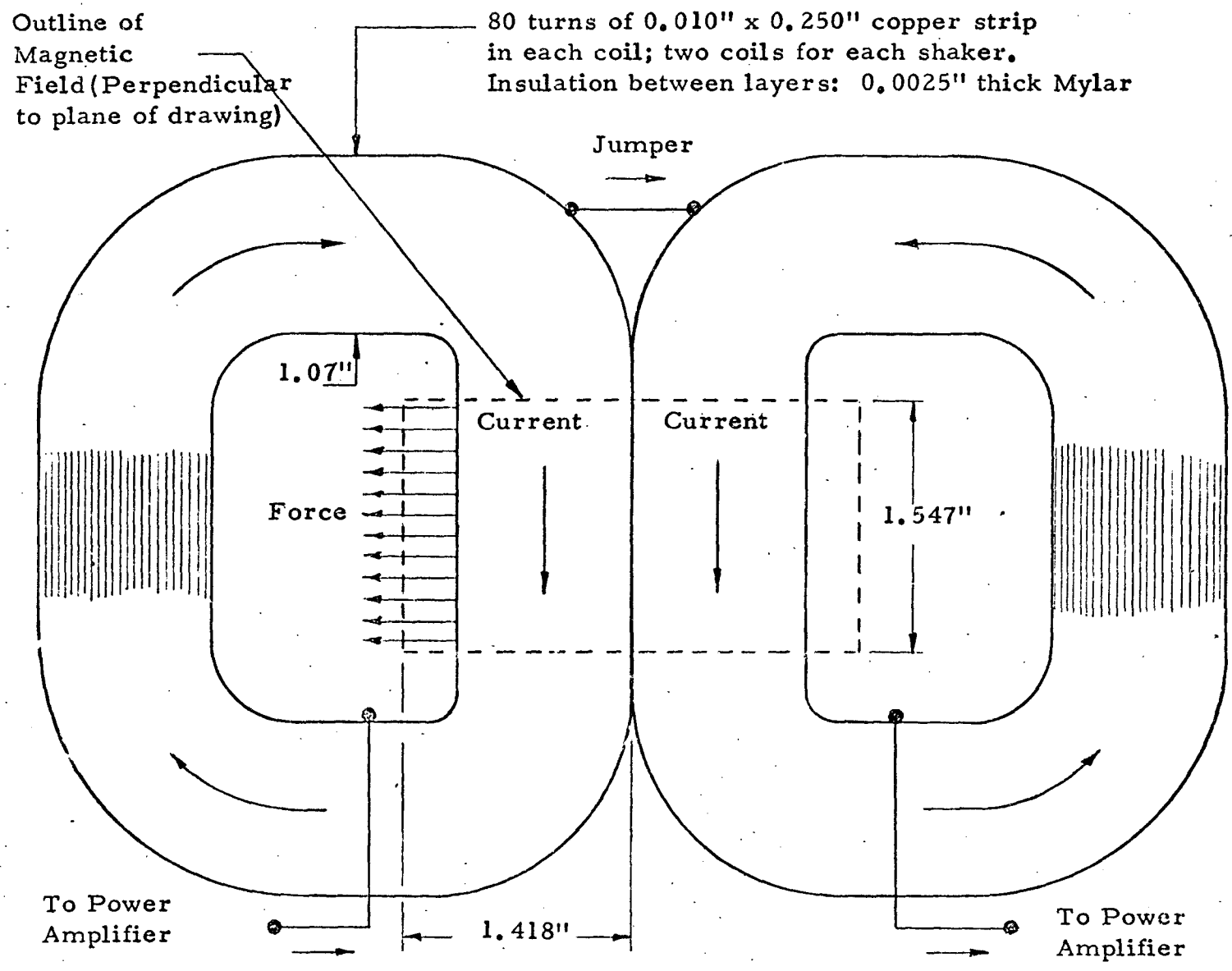

Figure 2 Force Coil Configuration

Conductor: 0.010" x 0.250" copper strip

Insulator: 0.0025" Mylar tape

The number of turns per coil is increased from 42 to 80. Each force generator still uses two coils. External dimensions of the new coils are shown in Figure 2. The coil carrier was redesigned to accommodate the new coils. Refer to ADRC Dwg No. 20031 for details of the new coil carrier, and 20032-Revision A for the force coil assembly.

3.4 Other Damper Modifications

The method to attach four of the 12 coil springs which keep the damper centered with respect to the model was modified. This change is indicated in ADRC Dwg No. 20021-Revision B (Item 33).

3.5 Relative Velocity Sensor

In accordance with the results and conclusions of a stability analysis of the active damper system (see Section 4.1) a velocity sensor was developed for measuring the relative velocity between the model and the field magnet.

In order to measure relative velocity in two directions over a $\pm$ 0.35" stroke, a magnet-search coil design much like the damper is adapted. Only one field magnet is used in the velocity sensor, however, as search coils are made by printed circuit techniques and are sufficiently thin for both to fit into the same magnetic gap.

The field magnet of the velocity sensor consists of two ceramic permanent magnets. Pole pieces and a flux return circuit are made of a relay steel. The field magnet assembly is mounted on top of the upper electromagnet of the damper, as shown in Figure 3. Details of the relative velocity sensor, and its relationship with respect to the damper and the model are shown in ADRC Dwg 20033-Revision A.

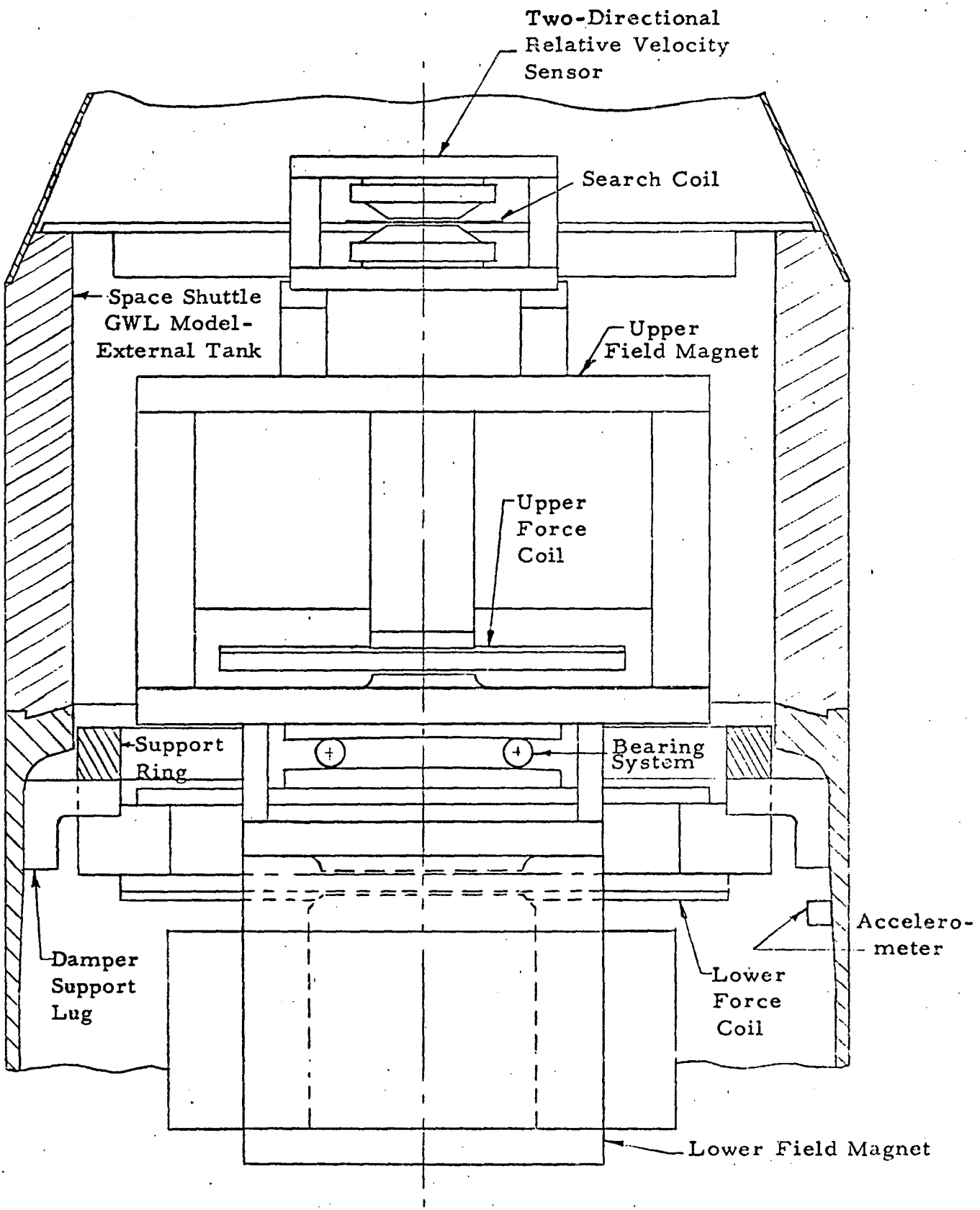

Fig 3 Damper-Model-Velocity Sensor Assembly

As mentioned earlier, the search coils are fabricated with standard printed circuit technology. Both sides of the pc card are used, one for each direction of motion. Twenty turns of printed conductors are used on each side. Other details of the search coils are shown in Figure 4.

Measured sensitivity of the relative velocity sensor is 5.88 mv/(in/sec) over the linear range of $\pm$ 0.35".

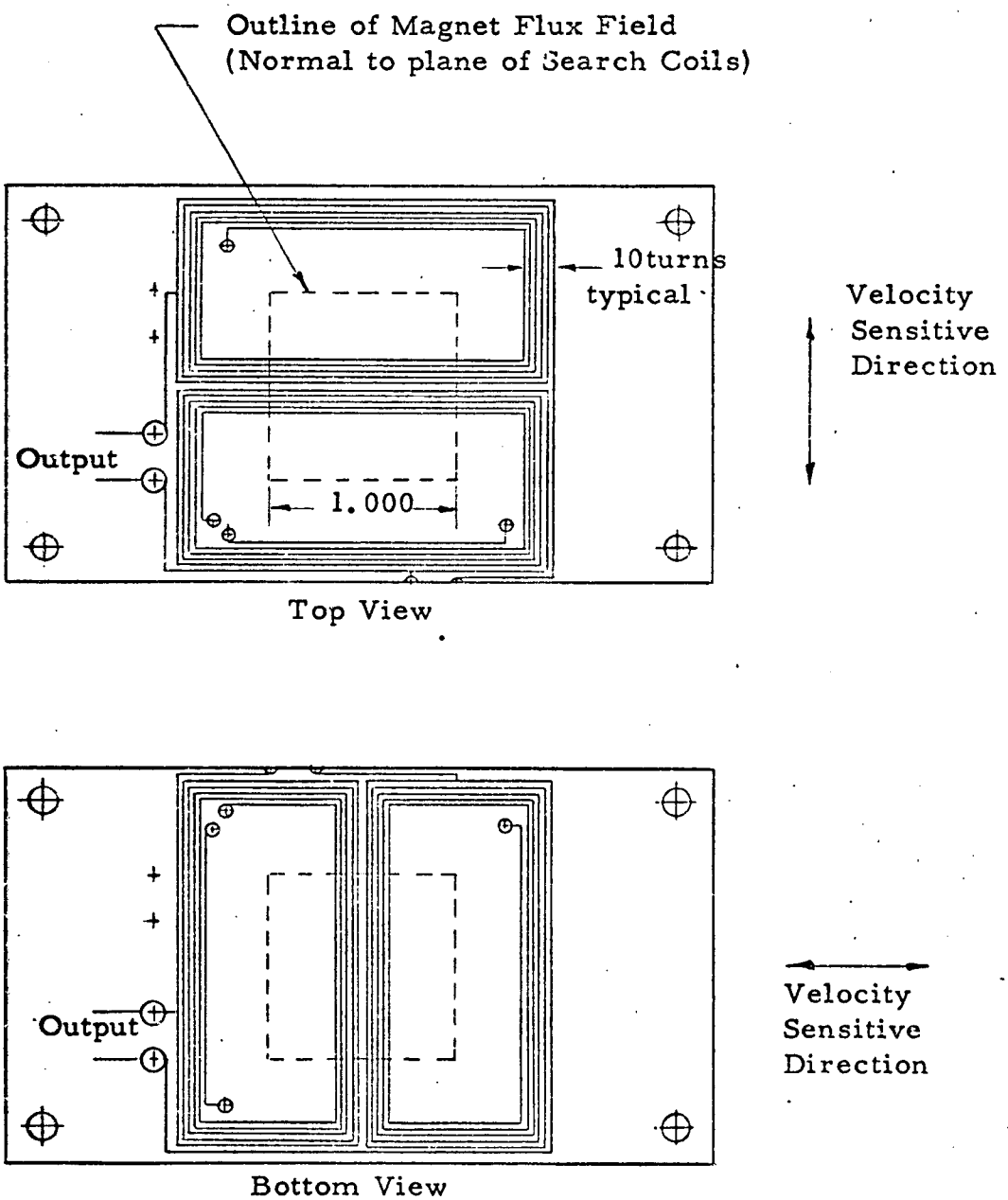

Fig 4 Velocity Sensor Search Coil

Section 4

DAMPER CONTROL SYSTEM

4.1 Stability Analysis

In previous GWL test programs, the active damper system usually displayed tendencies to become unstable (to go into a self-sustained oscillation) when simulation of high damping coefficients were required. The basic cause of this problem is established in the following analysis.

The aeroelastic model and the damper system are modeled structural dynamically in Figure 5. The field magnets of the force generators are modeled as rigid masses connected by a flexible connecting structure. In the pitch-plane, the location of the response transducer is specified by the position coordinate x_2. The damper force + F is applied to the model at the point x_o, and -F is applied to the pitch field magnet whose position coordinate is x_1. In the yaw plane, the transducer location is at x_2', the damper forces are $\pm F'$, and their points of application are x_o' and x_1'. Modal analyses will be used, and the first three mode shapes are sketched in Figures 6a (pitch modes) and 6b (yaw modes). In the following discussion, we will not distinguish pitch and yaw responses, and the unprimed variables only will be used in the equations.

The relationships among the response velocities (v_1 and v_2), the UAF (E), the modal characteristics (G_n, Φ_{n1}, and Φ_{n2}), the modal responses (v_{n1} and v_{n2}), the feedback gain (k), the damper forces ($\pm F$) and the generalized forces (E_n) are shown in Figure 7 in block diagram form.

The UAF is expandable into a modal series:

$$E(x_1 t) = \sum_n E_n'(t)$$

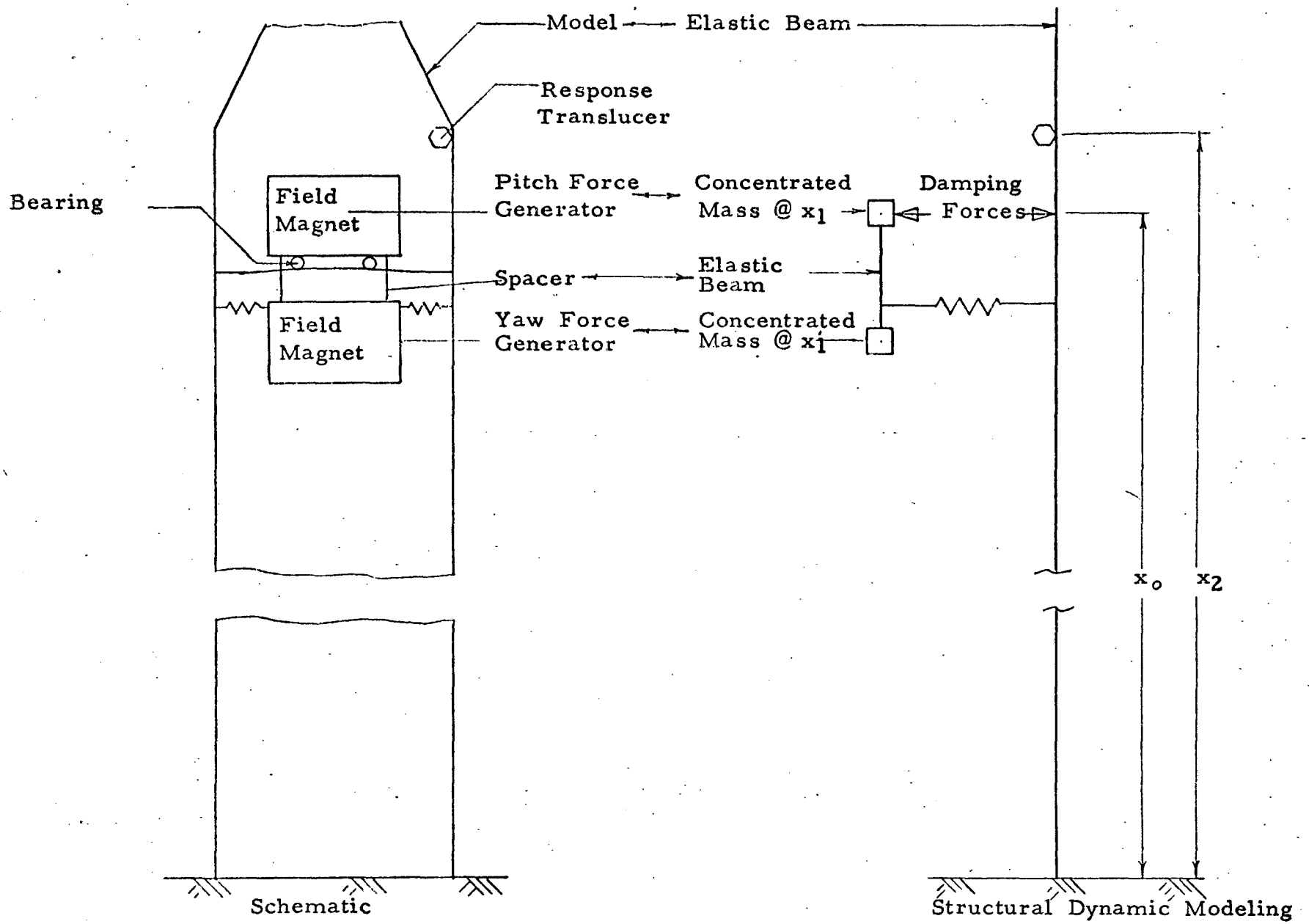

Fig 5 Structural Dynamic Modeling

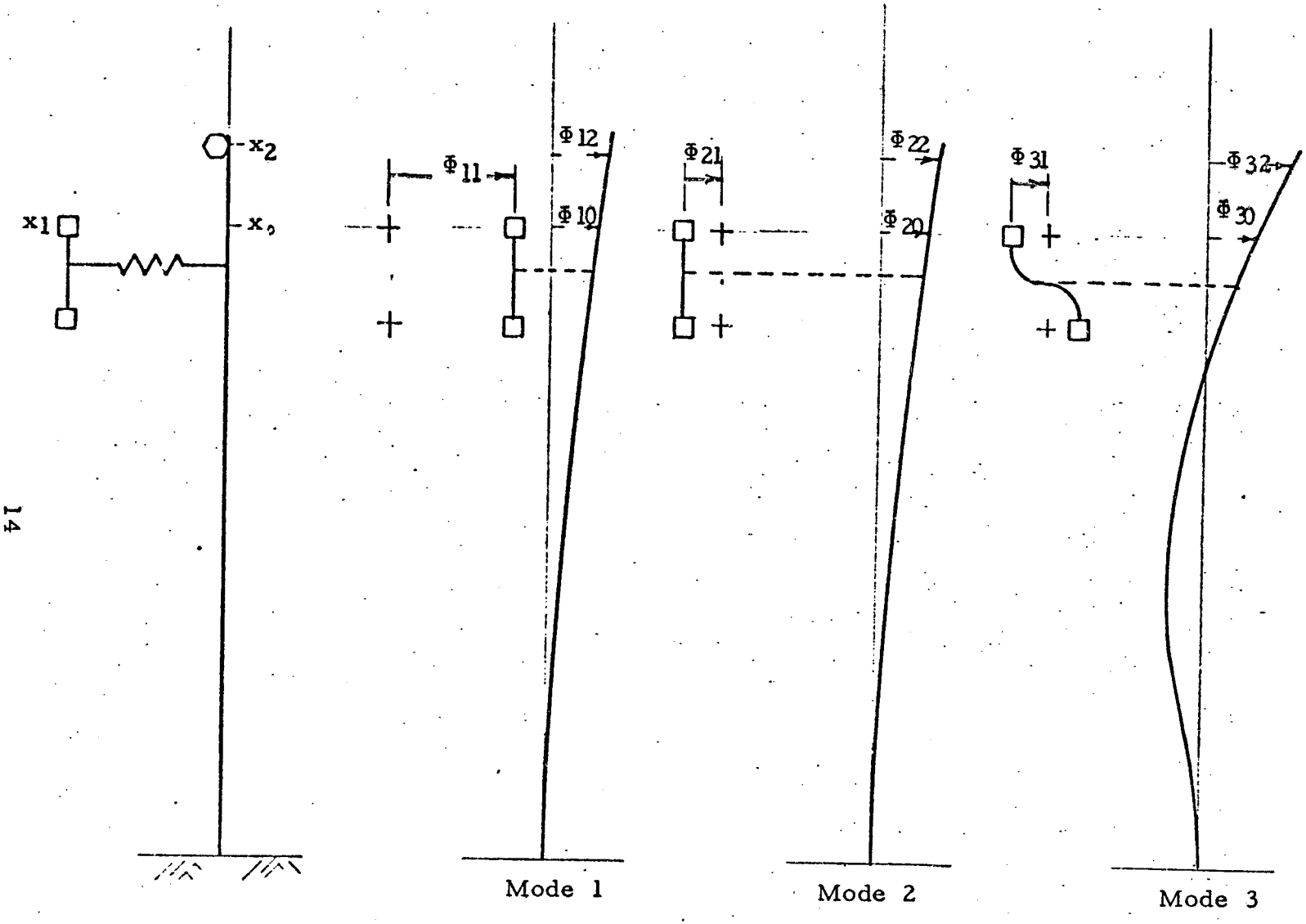

Fig 6a Pitch Mode Shapes

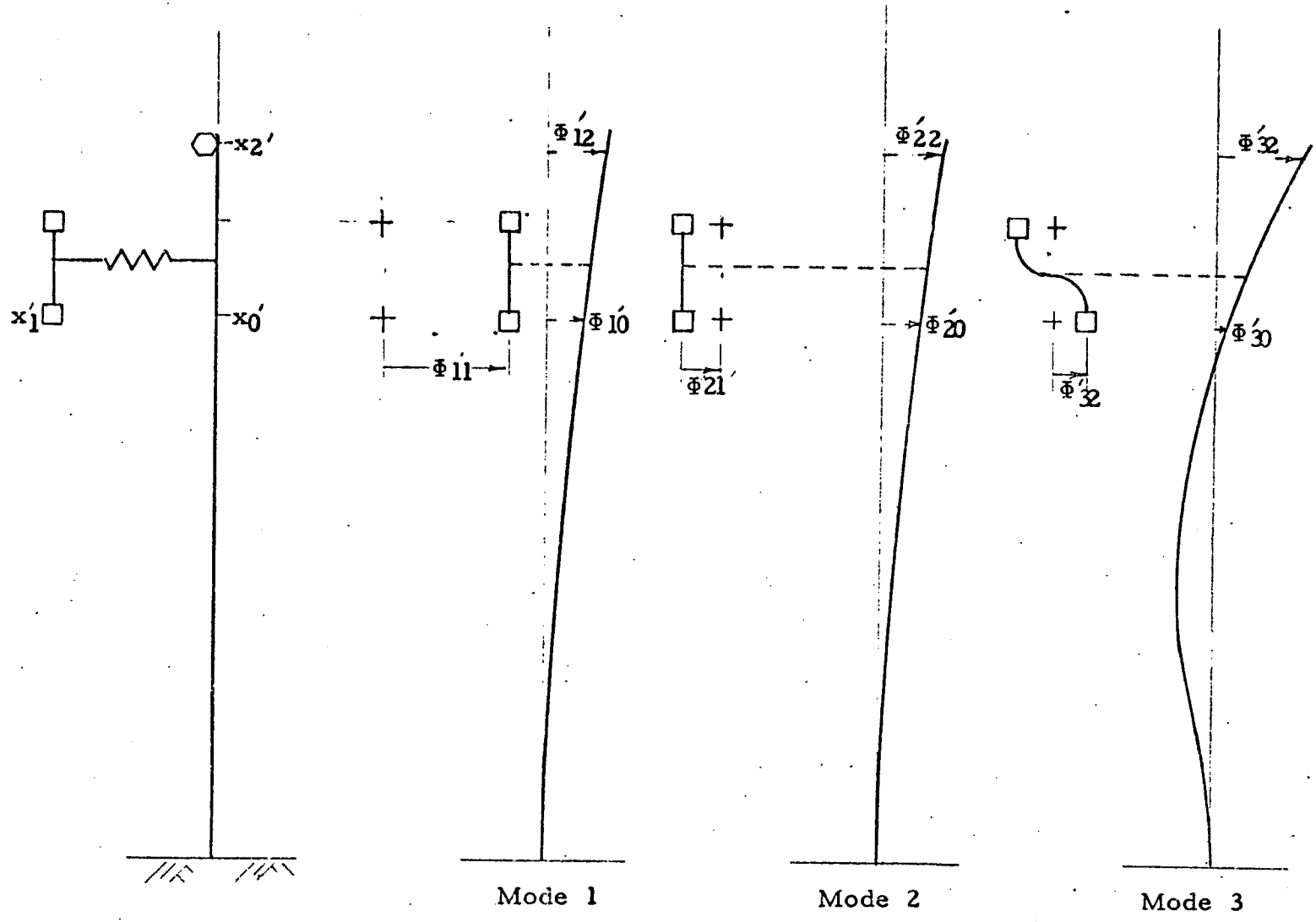

Fig 6b Yaw Mode Shapes

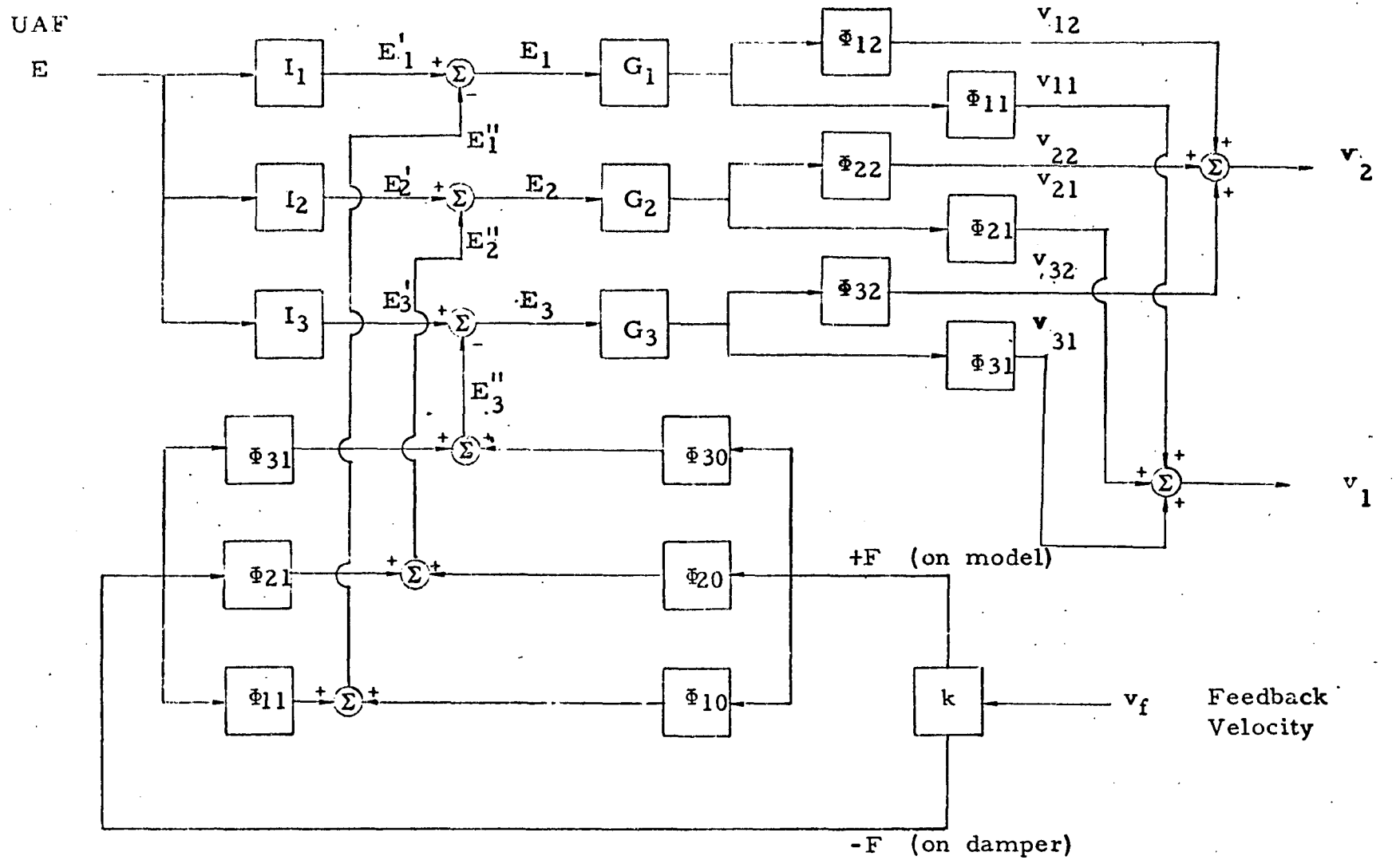

Fig 7 Block Diagram Representation of Aeroelastic Model with Active Damper

The damper force on the model carries a positive sign. Its contribution to the generalized forces in the n^{th} mode is $F(t)\Phi_{no}$. The damper force on the field magnet carries a negative sign and its contribution to the generalized force in the n^{th} mode is $-F(t)\Phi_{n1}$. The total generalized force in the n^{th} mode is

$$E_n(t) = E_n'(t) + F(t)\,(\Phi_{no} - \Phi_{n1})$$

After Laplace transformation, the response of the model as seen by the transducer located at $x = x_2$ is

$$\begin{aligned} v_2(S) &= \sum_n v_{n2}(S) \\ &= \sum_n E_n(S)\, G_n(S)\Phi_{n2} \\ &= \sum_n \left[E_n'(S) + (\Phi_{no}-\Phi_{n1})\, F(S)\right] G_n\Phi_{n2} \\ &= k(S)\, v_f(S) \sum_n \Phi_{n2}\,(\Phi_{no}-\Phi_{n1})G_n(S) + \sum_n \Phi_{n2}E_n'(S)G_n(S) \end{aligned}$$

The last term in the above equation is the response at x_2 of the model-damper due to the UAF alone (damper inactive). If $v_2(S)$ is used as the feedback signal, i.e., if we set

$$v_2 = v_f,$$

The expression for the closed-loop response is

$$v_2 = \frac{\sum_n \Phi_{n2}E_n'(S)G_n(S)}{1 + k(S)\sum_n \Phi_{n2}(\Phi_{n1}-\Phi_{no})G_n(S)}$$

At or near the natural frequency of the m^{th} mode, the magnitude of G_m becomes significantly greater than all others, and

$$v_2(S) \approx \frac{\Phi_{m2} E_m'(S)\, G_m(S)}{1 + k(S)\Phi_{m2}(\Phi_{m1}-\Phi_{mo})G_m(S)} \qquad @ \quad \omega \approx \omega_m$$

Let the generalized mass be M_m and the modal damping coefficient corresponding to inherent structural damping be ζ_m. Then

$$v_2(S) \approx \frac{\Phi_{m2} E_m'(S)\, S/M_m(S^2 + 2\zeta_m\omega_m S + \omega_m^2)}{1 + k(S)\Phi_{m2}(\Phi_{m1}-\Phi_{mo})S/M_m(S^2+2\zeta_m\omega_m S+\omega_m^2)}$$

$$= \frac{\Phi_{m2} E_m'(S)\, S}{M_m[S^2+2(\zeta_m+\zeta_m')\omega_m S + \omega_m^2]} \qquad @ \quad \omega \approx \omega_m$$

The effect of feedback on the model response is clearly the increase of modal damping from ζ_m to $(\zeta_m + \zeta_m')$, where

$$\zeta_m' = k(S)\ \Phi_{m2}(\Phi_{m1} - \Phi_{mo})/2M_n\omega_n$$

$$@ \quad \omega \approx \omega_m$$

If, in the course of adding positive damping to the n^{th} mode, the product $k(S)\Phi_{m2}(\Phi_{m1}-\Phi_{mo})$ is negative for another mode (the m^{th} mode), instability can occur when the feedback gain is raised sufficiently high to make the total damping in the m^{th} mode less than or equal to zero.

For GWL applications, damping in the second system mode (the first vehicle bending mode) is of primary interest. From the sketches in Figure 6a, we see that $\Phi_{22}(\Phi_{21}-\Phi_{20})$ and $\Phi_{12}(\Phi_{11}-\Phi_{10})$ have opposite signs. We may, therefore, conclude that unless k(S) changes sign between $\omega \approx \omega_1$ and $\omega \approx \omega_2$, the first mode (corresponding to large deflections of the force generator magnets) can easily become unstable.

Furthermore, the system can be unstable for those high-frequency modes having an odd number of node points on their mode shapes between x_2 and x_o. If the response transducer is located right at the point of damper force application, all high-frequency instability problems will be eliminated.

The ideal situation, however, is achieved when a relative velocity sensor is used to measure the quantity $v_o - v_1$ and use it as the feedback signal. In that case,

$$
\begin{aligned}
v_f &= v_o - v_1 \\
&= \sum_n [v_{no}(S) - v_{n1}(S)] \\
&= \sum_n E_n(S)G_n(S)(\Phi_{no} - \Phi_{n1}) \\
&= \sum_n [E_n'(S) + (\Phi_{no} - \Phi_{n1})E_d(S)](\Phi_{no} - \Phi_{n1})G_n(S) \\
&= k(S)[v_o(S) - v_1(S)] \sum_n (\Phi_{no} - \Phi_{n1})^2 G_n(S) \\
&\qquad + \sum_n (\Phi_{no} - \Phi_{n1})E_n'(S)G_n(S)
\end{aligned}
$$

or

$$
v_o(S) - v_1(S) = \frac{\sum_n (\Phi_{no} - \Phi_{n1})E_n'(S)G_n(S)}{1 + k(S) \sum_n (\Phi_{n1} - \Phi_{no})^2 G_n(S)}
$$

The additive damping is

$$\zeta_n' = k(S)\,(\Phi_{n1} - \Phi_{no})^2 / 2M_n\omega_n$$

for all n. Variation of mode shape from mode to mode cannot change the polarity of ζ_n' because the factor involving mode shape is squared. The feedback gain, therefore, can be simply a constant with respect to frequency.

For the Space Shuttle program, a relative velocity sensor was developed and placed immediately above the pitch force generator. For all practical purposes, the above-mentioned ideal situation was achieved for the pitch channel and a constant (with respect to frequency) feedback gain was useable. For the yaw channel, however, complications arose because of the elastic deformation between the relative velocity sensor and the yaw (lower) field coil in the third mode (refer to Figure 6b). Using the relative velocity sensor alone, it was found impossible to stablize both the first and the third modes simultaneously. The final approach adapted for the yaw channel is shown in Figure 8. A low-pass filter was used to eliminate the destablizing effect of the relative velocity signal on the third mode. Damping in the second mode (the mode of primary interest) was achieved via the usual accelerometer-plus-integrator approach. High frequency instability was not a significant problem. The frequency of the oscillation, when it ultimately occured, was extremely high. The instability was easily suppressed with a 0.01 uf feedback capacitor in the high-gain stage. See Figure A-3.

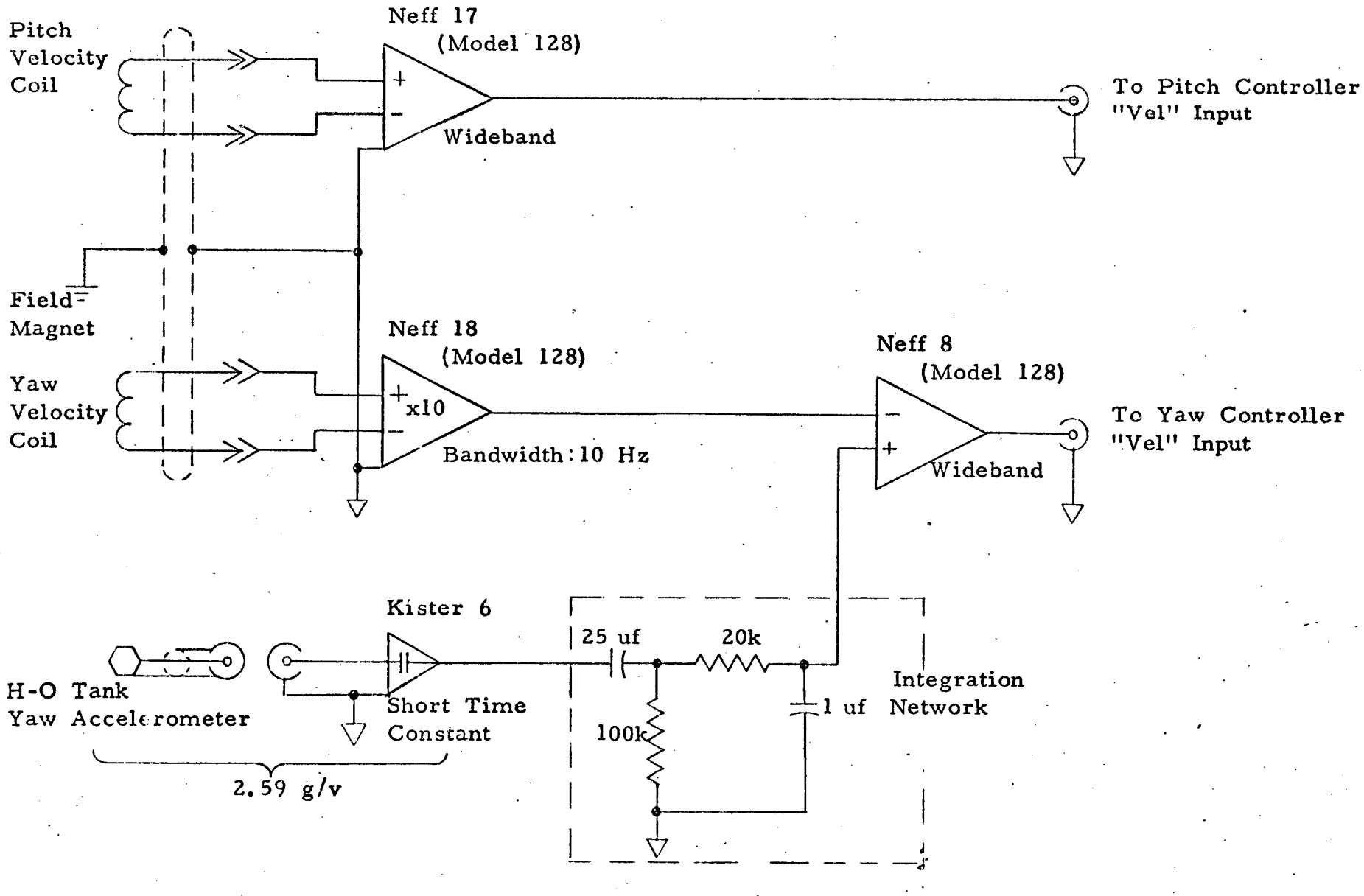

Fig 8 Damper Control Instrumentation

4.2 Control System Description

A separate, independent controller was fabricated for each damper channel. Each controller contains its own power supply (Figure A-1, Appendix A) and a null meter for pre-test self checking (Figures A-2 & A-3). In addition to providing damping gain control and power amplifier drive voltages, each controller also includes a means of mixing a sinusoidal signal obtained from an external source (a Voltage Controlled Function Generator) for conducting vibration check-out tests of the wind tunnel model. Figure A-3 is an over-all schematic of the controller. A voltage limiter is built into the controller to avoid accidental over-current in the power amplifier output to occur. The limiter is shown in details in Figure A-4. The frequency of the mixed sinusoidal signal can be fine-tuned from each controller using the circuit of Figure A-5. In addition, an electronic zero-crossing switch is incorporated also to switch off the sinusoidal excitation signal from the VCF for conducting damping decay tests. A logic circuit was developed to accomplish this using either controller.

4.3 Power Amplifier

The force generators were driven by two Unholtz-Dickie TA-100 power amplifiers. The input stages were modified to provide an over-all voltage gain of 10 (Figure A-6). The 3-phase and single-phase a.c. power are controlled by the Power Control Panel (Figure A-7) which provides malfunction protection in conjunction with relays internal to the TA-100's.

Power amplifier output connection and current sensing are incorporated in the Power Connector Panel (Figure A-8). Field power supply (d.c. @ 20 amps for each field magnet) are also provided through this interface.

4.4 Current Feedback

After the wind tunnel test program was completed, "current feedback" circuits were installed in the Damper Controllers to improve the performance of the system as vibration test equipment. Schematics of current sensing and feedback circuits are included in Figures A-3 and A-8 of Appendix A.. Figure 9 is a summary of the current feedback circuit.

4.5 Damper Operating Conditions

During "wind-on", the operating conditions for the damper system were the following:

(a) Field current: 2.0 amps, d.c., each channel

(b) Cooling: Freon at 12 psig

(c) Recorded* Signals: Control velocity, pitch
Control velocity, yaw
Damper current, pitch
Damper current, yaw

When the turntable was being operated to change the test azimuth, the damper controls must be set to maximum damping level to prevent the field magnet assembly from impacting on the model.

---

* On oscillograph

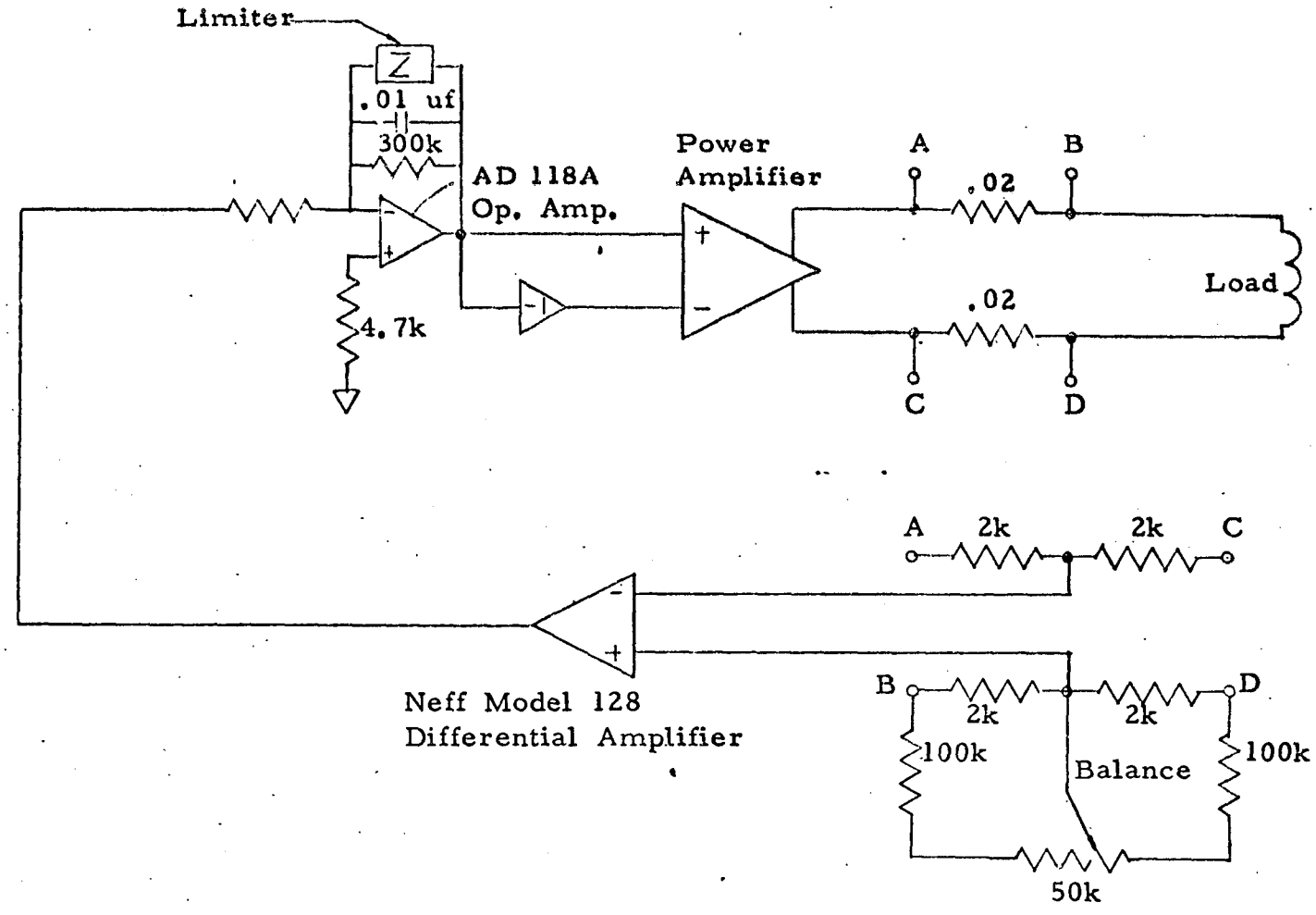

Fig 9 Current Feedback Schematic

Section 5

INSTRUMENTATION

Damper control system electronics and a number of vibration and wind tunnel test equipment are assembled together in a standard two-bay instrumentation rack. Capabilities for transducer signal conditioning, calibration, data monitoring, measuring, recording and interfacing with external equipment are included. This instrumentation system was used for (1) conducting vibration checkout tests of the Space Shuttle model in the laboratory and when the model was set up in the wind tunnel; (2) setting up and distributing d. c. and a. c. calibration signals for magnetic tape and oscillographic recorders; (3) conditioning most of the model response transducer signals during wind tunnel tests; and distributing the conditioned signals to recorders and an on-line data analysis system; and (4) providing real-time display of critical transducer signals for monitoring model safety. The following is an item-by-item description of this instrumentation system.

5.1 Strain Gage Signal Conditioners

Ten channels of Incor Instrumentation's strain gage conditioning equipment are included in the system. Each channel consists of a Model 215A Isolated Power Supply and a Model RB-2 Balance and Calibration Module. Five units of each are combined alternately in a 19-inch case. The cases are located approximately half way up in the right-hand bay of the rack, see Figures 10 and 11.

Power supply voltages are individually adjustable for each channel. Voltage adjustment control and a voltage monitor jact are located on the front panel of each Model 215A. The Model RB-2 is installed immediately adjacent to the power supply and no external connections are required between them. In addition to providing a bridge balance control, the front panel also includes four push-button switches for two levels of shunting of two opposite arms (separately) of a strain gage bridge.

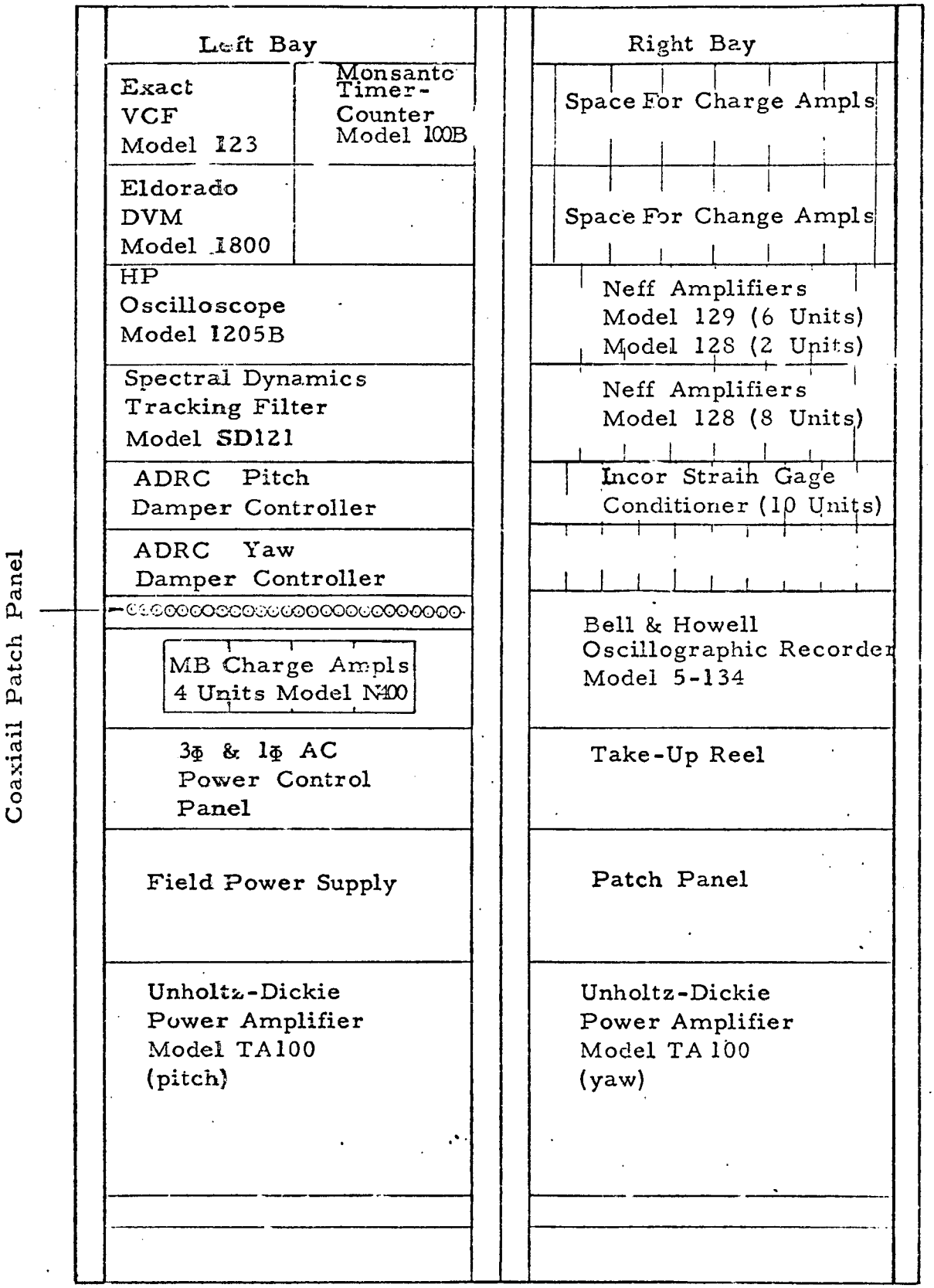

Fig 10 Control and Instrumentation System Assembly-Front View

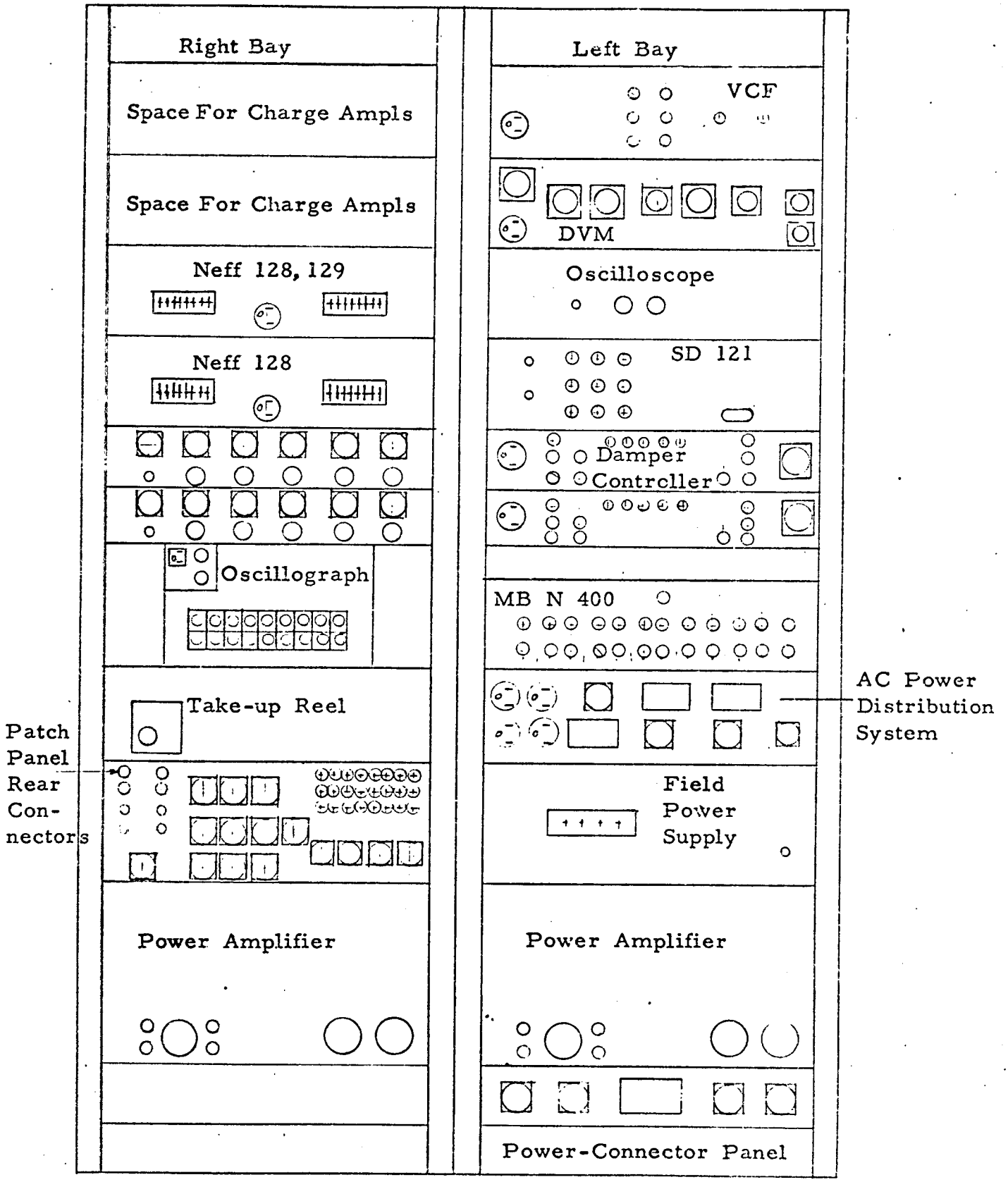

Fig 11 Control and Instrumentation System Assembly-Rear View

Bridge completion and shunt resistors are user-installed on the inside of the RB-2. All transducer and data amplifier connections are made through connectors located on the rear panel. Figure 12 is a schematic diagram of a typical 4-arm strain gage instrumentation channel.

5.2 D. C. Data Amplifiers

Ten channels of Neff Model 128 Wideband Differential Amplifiers and six channels of Neff Model 129 D-C Amplifiers are included in the instrumentation rack. They are installed directly above the INCOR strain gage conditioners.

In the Space Shuttle GWL application, Model 128's were used for amplifing strain gage signals, relative velocity sensor signals, and for summing of two signals from different sources (as in damper control). Twelve fixed gain steps of 0.2, 0.5, 1, 2, 5, 10, 20, 50, 100, 500 and 1,000 are switch selectable for the Model 128. In addition, a variable gain multiplier is also provided for an over-all continuous gain adjust range from 0.2 to 2,500.

A switch selectable, 12dB/Octave low pass Bessel filter is included in the Model 128, providing a selection of cut-off frequencies of 10 Hz, 100 Hz, 1 K Hz, 10 K Hz and 50 K Hz(wideband).

Input to the Model 128 are made through a floating, guarded connector directly onto the main p.c. card. Voltage and galvonometer driving outputs are available from the amplifier. The voltage output from all Model 128's are connected to the patch panel for distribution. Details of this arrangement will be described in Section 5.6.

The Model 129 D-C Amplifiers have single-ended inputs and are primarily useful as galvo drivers, buffer-amplifiers and amplification of high level signals. In the Space Shuttle GWL program, two Model 129's were used for amplifying outputs of force coil current sensing bridges, two were used for amplifying and buffering dynamic model response

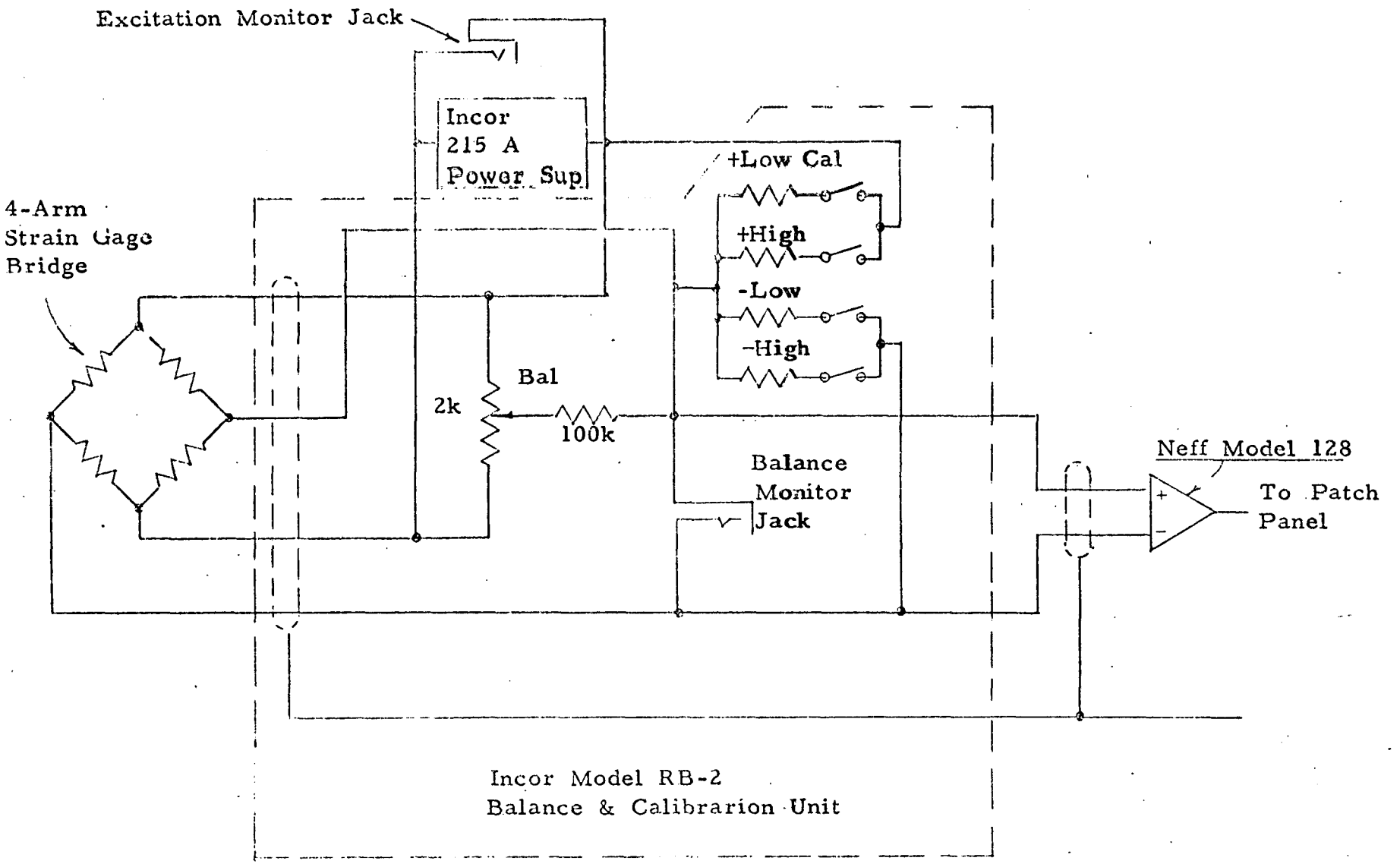

Fig 12 Strain Instrumentation Schematic

signals for log conversion and recording, one was used to provide a. c. calibration signals to two tape recorders and an oscillographic recorder and one was left as spare.

Both the input and the output connections to the model 129 are arranged through the Patch Panel.

5.3 Charge Amplifiers

A total of 16 charge amplifiers were assembled in the instrumentation rack for conditioning piezo-electric accelerometer output signals. These were of three types, Kistler Model 504 (6 channels), Kistler Model 566 (6 channels) and MB Model N400 (4 channels).

The Kistler units were obtained through a loan arrangement for the duration of the Space Shuttle GWL test program only. The two Kistler models are identical in size and are mounted in the space above the Neff Amplifiers. Their outputs are direct-coupled and severe d. c. level drift problems were encountered during the wind tunnel test program. After repeated attempts to eliminate the drift with the built-in adjustment had failed, a. c. coupling of the output with the recorders had to be installed. This was accomplished by inserting a capacitor in the patch cord which distributes the output signal.

The MB N400 Charge Amplifiers were acquired during a previous GWL program (Reference 1) and are permanent parts of the instrumentation system. They are installed in the left-hand bay of the rack, approximately waist-high. Two of these charge amplifiers were used for vibration checkout test only. The remaining two units were used for wind tunnel tests also.

Charge amplifier inputs were made directly on the back of each unit through Microdot-BNC connectors. All charge amplifier outputs are connected to the Patch Panel for distribution.

5.4 Tracking Filter

A Spectral Dynamics Model SD121 Tracking Filter is included in the instrumentation system. It is located between the oscilloscope and the Damper Controller, in the left-hand bay. Two filter bandwidths are available 1.0 Hz and 10 Hz. The filter shape factor is 5.6 to 1 (- 60dB bandwidth to -3dB bw). The 1-Hz filter was used throughout the vibration and wind tunnel tests.

The center frequency of the filter is established by a sinusoidal "tuning" signal from the Voltage Controlled Function Generator (an Exact Model 123). Since during a vibration test all shaker excitation and model response frequencies are also established by the same sinusoidal source, the Tracking Filter is useful for measuring the fundamental components of these signals. In addition, the phase difference between the input and the output signals of the filter can be accurately adjusted to an even multiple of 360° over a wide range of center frequencies. It is, therefore, very useful for determining natural frequencies of a vibration system using an x-y display of the force and response signals on an oscilloscope screen.

A dc voltage proportional to the amplitude of the filtered signal is available from the SD 121. This feature provides an accurate and convenient readout on a digital voltmeter of a.c. voltage amplitudes for frequencies as low as 1 Hz.

During the Space Shuttle GWL program, the SD 121 was connected according to the schematic diagram shown in Figure 13. The arrangement was found to be very convenient for nearly all phases of the test program.

5.5 Other Equipment

The following equipment are also included in the control-instrumentation system: (1)

(1) An Exact Model 123 Voltage Controlled Function Generator which is the signal source for all vibration tests, calibration voltages, and the tuning signal for the SD 121 Tracking Filter. Extremely fine resolution in

Note(a): Filter must be "out" for Log conversion and for reading dc input voltages

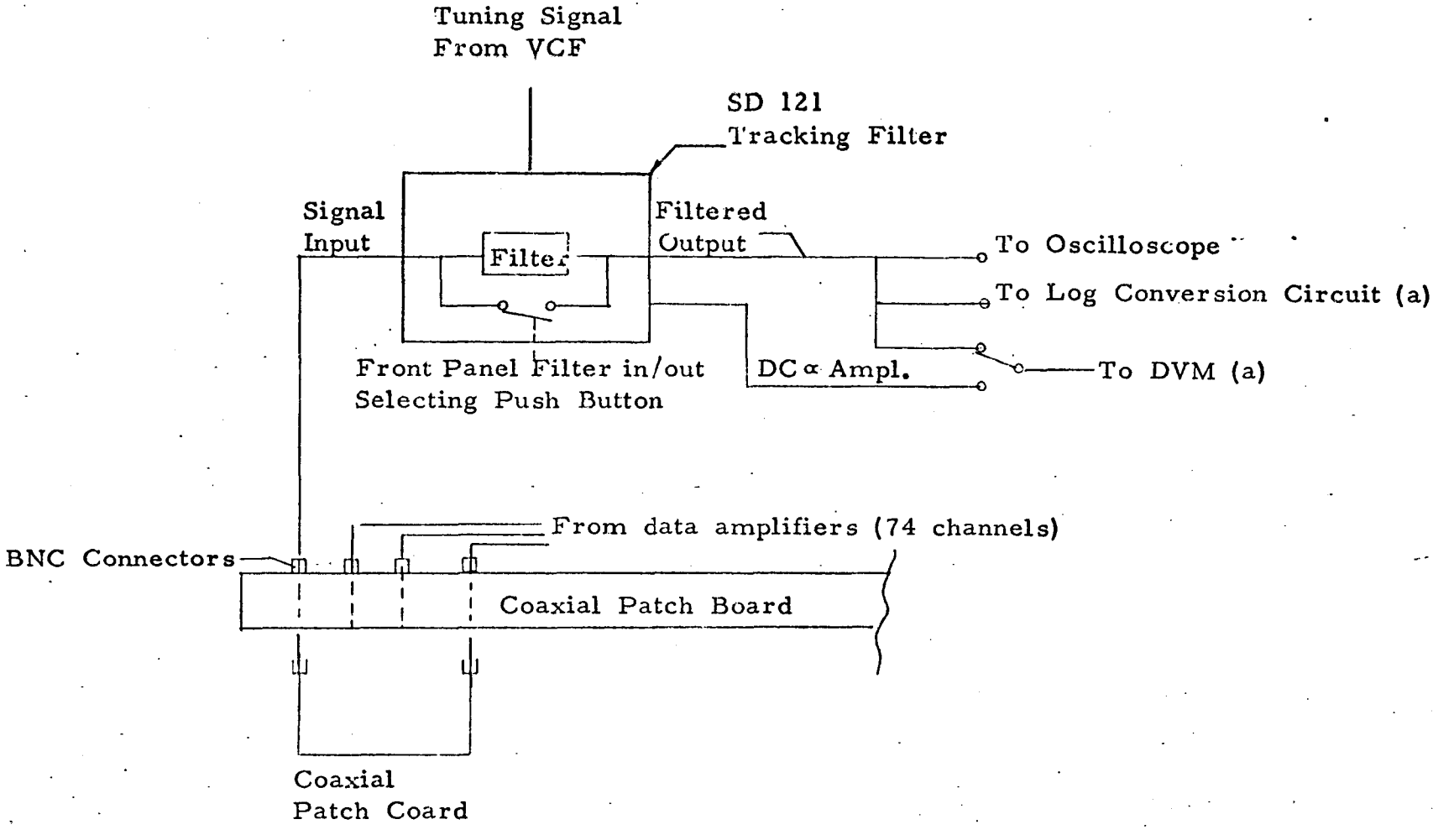

Fig 13 Tracking Filter Arrangement

frequency adjustment was achieved by the regulated control voltage from the Damper Controller.

(2) A Monsanto Model 100B Electronic Counter-Timer for accurate determination of the frequency of the VCF output

(3) An Eldorado Model 1800 Digital Voltmeter

(4) A Hewlett-Packard Model 1205B Oscilloscope

(5) A Bell & Howell Model 5-134 Oscillograph with a take-up reel and 12 Model 7-316 Galvonometers.

5.6 Patch Panel

All signals except low-level transducer outputs and a few critical damper control voltages are channeled through the Patch Panel which is located above the power amplifier and below the oscillograph in the right-hand bay of the instrumentation rack. Patching is accomplished in the front. Removable plug-in patchboards are used so that a number of different test setups can be patched (one on each board) and checked out beforehand for quick interchangeability.

All connections to the patch points are made through connectors located on the rear panel of the Patch Panel chasis. BNC and MS types of connectors are used. All internal wiring (from the rear receptables to the patch points) use RG 174/U coaxial cables. The patch cords are, however, single-conductor cords.

Patch Panel schematics (patch point identifications) are included in Appendix B of this report.

5.7 Coaxial Patch Panel

A 26-point coaxial patch panel is used for selection of monitor signals. This facility is located in the left-hand bay, below the Damper Controllers.

5.8 Interface

During wind tunnel tests, conditioned accelerometer and strain gage instrumentation signals were distributed to data recorders and an on-line analyzer. All signals were channeled through the Patch Panel and Rear Connectors H and F.

Section 6

MODEL AND SYSTEM CALIBRATION

6.1 Dynamic Calibration Tests

During the wind tunnel test program, a significant amount of dynamic calibration tests were conducted with the model setup in the wind tunnel. A total of 13 model configurations were used. For each configuration the following dynamic calibrations were conducted.

(1) Natural frequencies - Model natural frequencies below 150 Hz were determined.

(2) Mode shapes - For each natural frequency determined above, the mode shape was measured. Fixed and roving accelerometers were used.

The first mode* for all configurations is a bending mode of the H-0 Tank (External Tank) in the pitch plane. The second mode is a bending mode of the H-0 Tank in the yaw direction. The third mode is a torsional mode of the system. The natural frequencies for these three low-frequency modes were directly governed by the base stiffness and the simulated fuel levels.

The fourth, fifth and six modes are the pitch, yaw and roll modes of the Orbiter on the tie rods which connect it to the H-0 Tank. The natural frequencies for the "Orbiter modes" vary according to the stiffness of the tie rods used, and the payload simulation and are not always in the order given above.

(3) Generalized Mass

The generalized mass for each of the three low-frequency modes were determined by adding small concentrated weights to the model and measuring the variation of the natural frequency due to the additions. The

* The numbering of the modes in this section is different from that used in Section 4. The actual first mode of the model-damper system is approximately 1 Hz in which the damper moves significantly. Such damper modes, however, could not be excited by the UAF to any significant magnitude and were disregarded during model calibration test.

procedure was well established for low-frequency modes and are described in, for example, Reference 3.

(4) Damping

Modal damping with and without addition from the damper system were determined for the fundamental bending modes for each wind tunnel test configuration. Variations of damping with respect to the wind tunnel azimuth were also checked out.

Damping for the Orbiter modes were measured in selected cases.

All dynamic calibration data were collected and analyzed by MSFC S&E-AERO-AUE.

6.2 Damper Calibration Test Setup

All damping calibration tests were conducted using the free-vibration technique. An Analog Devices Model 755N Logarithmic Converter was used to convert one-half (the negative voltages) of the exponentially decaying vibration signal to a logarithmic scale so that a linearly decaying record can be obtained on-line. The setup is shown in Figure 15. The Converter was tentatively installed in the Pitch Damper Controller to utilize its power supply during the wind tunnel test program. Afterwards, two channels of AD Model 755N were wired up in a separate chasis and installed in the instrumentation rack.

The gains of the buffer amplifiers used in the log conversion process were adjusted to yield a final scale factor of 10 dB/in on the oscillograph.

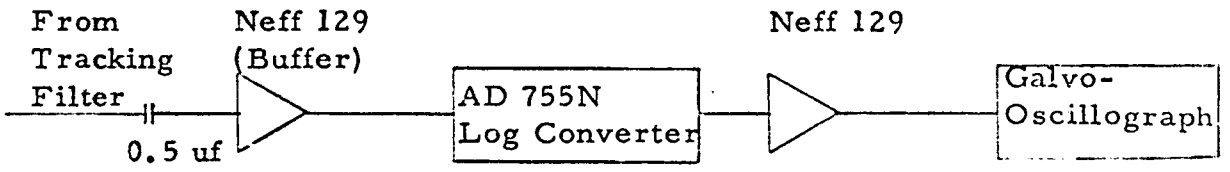

Figure 14 Log Conversion Schematic

6.3 Strain Gage Calibration

Two levels of strain gage bridges were installed on the lower section (Stations 6.25 and 21.25) of the H-0 Tank to measure total bending moment on the model in both the pitch and the yaw directions. Two additional sets of strain gages were installed in the same general area to measure torsion

Static calibration tests were conducted when the model was set up in Building 4619 at MSFC, prior to the beginning of the wind tunnel program. The following calibration results were obtained:

Sta. 6.25	Pitch Bending Gage Sensitivity:	16.87 in-lbs/ uv*
Sta. 6.25	Yaw Bending Gage Sensitivity:	17.83 in-lbs/ uv
Sta. 21.25	Pitch Bending Gage Sensitivity:	6.28 in-lbs/ uv
Sta. 21.25	Yaw Bending Gage Sensitivity:	6.03 in-lbs/ uv
	Torsion Gage (T 11) Sensitivity:	30.1 in-lbs/ uv

Based on the above calibration, the maximum allowable strain in each direction, the projected total strain to be experienced in the wind tunnel, and the maximum voltage for the magnetic tape recorders, shunt resistors of the following values were inserted in the Incor RB-2 Conditioner:

* Bridge excitation voltage was 10.00 volts d.c. as measured at the connectors at the base of the model.

± Pitch-Bending Shunt Resistances:

Sta. 6.25 Low Level - 121 K ohms	540	mv* =	45,540	in-lbs
Sta. 6.25 High Level - 49.9K ohms	1,304	mv =	109,970	in-lbs
Sta. 21.25 Low Level - 85.8K ohms	516	mv =	16,200	in-lbs
Sta. 21.25 High Level - 36.8K ohms	1,203	mv =	37,770	in-lbs

± Yaw Bending Shunt Resistances:

Sta. 6.25 Low Level - 121 K ohms	540	mv =	48,150	in-lbs
Sta. 6.25 High Level - 49.9K ohms	1,300	mv =	115,920	in-lbs
Sta. 21.25 Low Level - 85.8K ohms	516	mv =	15,570	in-lbs
Sta. 21.25 High Level - 36.8K ohms	1,201	mv =	36,230	in-lbs

± Torsion Shunt Resistance:

Low Level 5.0 M ohms	515	mv** =	83,170	in-lbs
High Level 2.0 M ohms	1,201	mv =	207,200	in-lbs

During wind tunnel setup, the excitation voltage from each Incor 315A Power Supply was adjusted individually until exactly 10.00 volts was measured at the connectors at the base of the model. The voltages required of the 315A to yield this condition were measured. These voltages were maintained at these levels throughout the wind tunnel test program.

For 120-ohm bridges, the required voltage at the power supply was found to be 10.408 volts; for 350-ohm bridges, the voltage was 10.139 volts.

---

* With Neff 128 gain set at 500
** With Neff 128 gain set at 2,905

6.4 Calibration Voltages For Recorders

Two 14-channel FM tape recorders were used during the test for wind tunnel model response signals. All data channels were adjusted to have a $\pm$ 1.4 volt recording range.

"Low Shunt" resistors were used to produce positive and negative d.c. voltages which were recorded on tape as a means of calibration.

A 1.00 V (zero-to-peak) sinusoidal signal was distributed to each recorder data channel for the same purpose. Two "AC CAL" frequencies were provided - 15.0 Hz and 100.0 Hz.

A single Neff Model 129 amplifier was used to drive all tape recorder channels simultaneously during AC CAL. Since the AC CAL was not supplied by individual data amplifiers, only partial calibrations of the data channels were provided.

Section 7

CONCLUSIONS AND RECOMMENDATIONS

Results of the analysis in Section 4.1 indicate that the instability of a GWL model with active damping is predominantly caused by improper selection of the type and location of the control transducer. The optimum transducer is a direct-coupled velocity sensor measuring the relative velocity of the field magnet and the point on the model where the damping force is applied. If this arrangement is physically realizable, the system will be completely stable. For the fundamental mode of the model-damper system, nodes are absent on the model in the vicinity of where damping forces are usually applied, and the field magnet assembly is essentially rigid. A relative velocity measurement between any point on the model and another on the magnets will be capable to stablize that mode. To avoid instability in high-frequency modes, the general rule to follow is to place the response transducer as close to the force generator as possible to avoid bracketing of a node between them.

Significant difficulties were encountered in determining and identifying high frequency modes of the Space Shuttle model. One of the major experimental constraints was the lack of a convenient means to apply well controlled, precisely known vibration excitations directly to the Orbiter without adding mass, damping and/or stiffness of non-negligible magnitudes. Dynamic properties of the system were, therefore, altered by the excitor itself. Furthermore, when the excitor had to be relocated to, say, better excite a new mode, other modes would be effected by the relocation and lose their identities, a situation which could have created additional confusion.

Two measures are recommended to overcome such difficulties in future programs: (1) develop small vibration excitors for installation of the Orbiter and the SRM's. These excitors should be designed and

considered as parts of the model. Their masses, damping and stiffnesses should be included in the model design (dynamic) analyses, so that the correct dynamic simulation is achieved with the inclusion of the excitors.

Another source of difficulty in determining high-frequency modes was possibly the coupling of otherwise orthogonal modes by non-proportional or heavy damping. The concept of using built-in excitors recommended above will also help to reduce the complexity of the problems of this origin--to a degree. An analytical investigation combined with analog and/or digital computer simulation of complex structures which are coupled by nonlinear and non-proportional damping mechanisms is recommended to establish guidance for better experimental and data analysis procedures in the future. In this regard, a preliminary research effort by Chang (Reference 4) in association with damping studies of a 20% model of the Saturn I launch vehicle appears to be a successful initial step in the right direction. Further research to expand the method developed in Reference 4 is recommended.

Lastly, on account of the high rate of zero drift, direct coupled charge amplifiers are not recommended for wind tunnel tests.

REFERENCES

1. Applied Dynamics Research Corporation Report No. T1008F, "Design, Develop, Fabricate, Assemble and Checkout an Active Damper System," Final Report MSFC Contract NAS8-26593, 31 March 1972.

2. McDonnel Douglas' Corporation Report MDC E0758, "Design and Fabrication of a Dynamically Scaled Space Shuttle Ground Wind Loads Model," by J. A. Zara and T. B. Sellers, Final Report MSFC Contract NAS8-26838, 15 February 1973.

3. Scott, L. P., "Redesign of Ground Winds Model and Damper System for the Saturn V/Dry Workshop Simulation," Final Report Contract NAS8-25319, LMSC-HRBC D225346, October 1971.

4. Chang, C. S., "Nonlinear Dynamic Analysis of Structures - Volume I Nonlinear Damping in Structures," Final Report, MSFC Contract NAS8-21435, June 1970.

APPENDIX A

DAMPER CONTROL SYSTEM SCHEMATICS

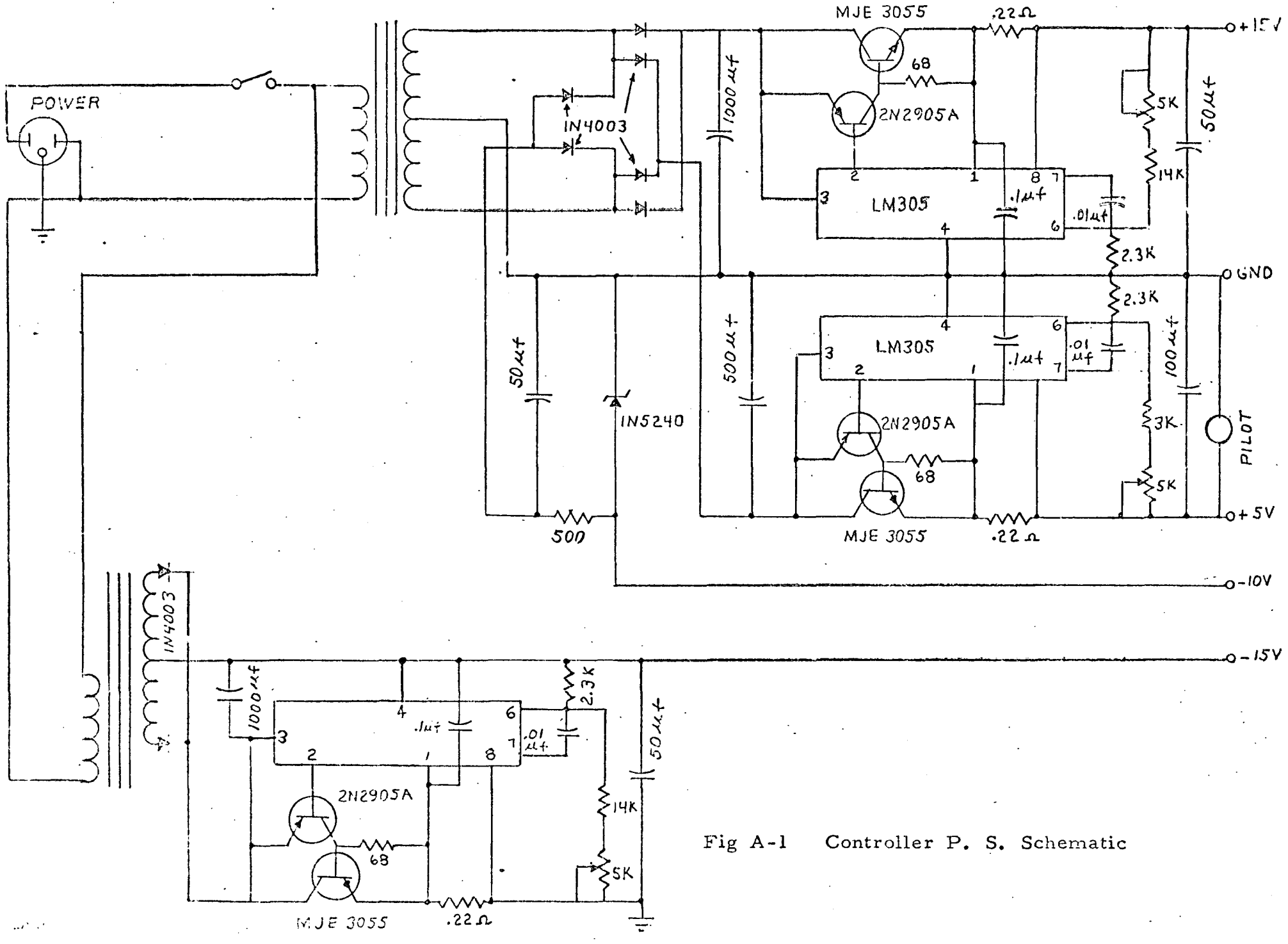

Fig A-1 Controller P. S. Schematic

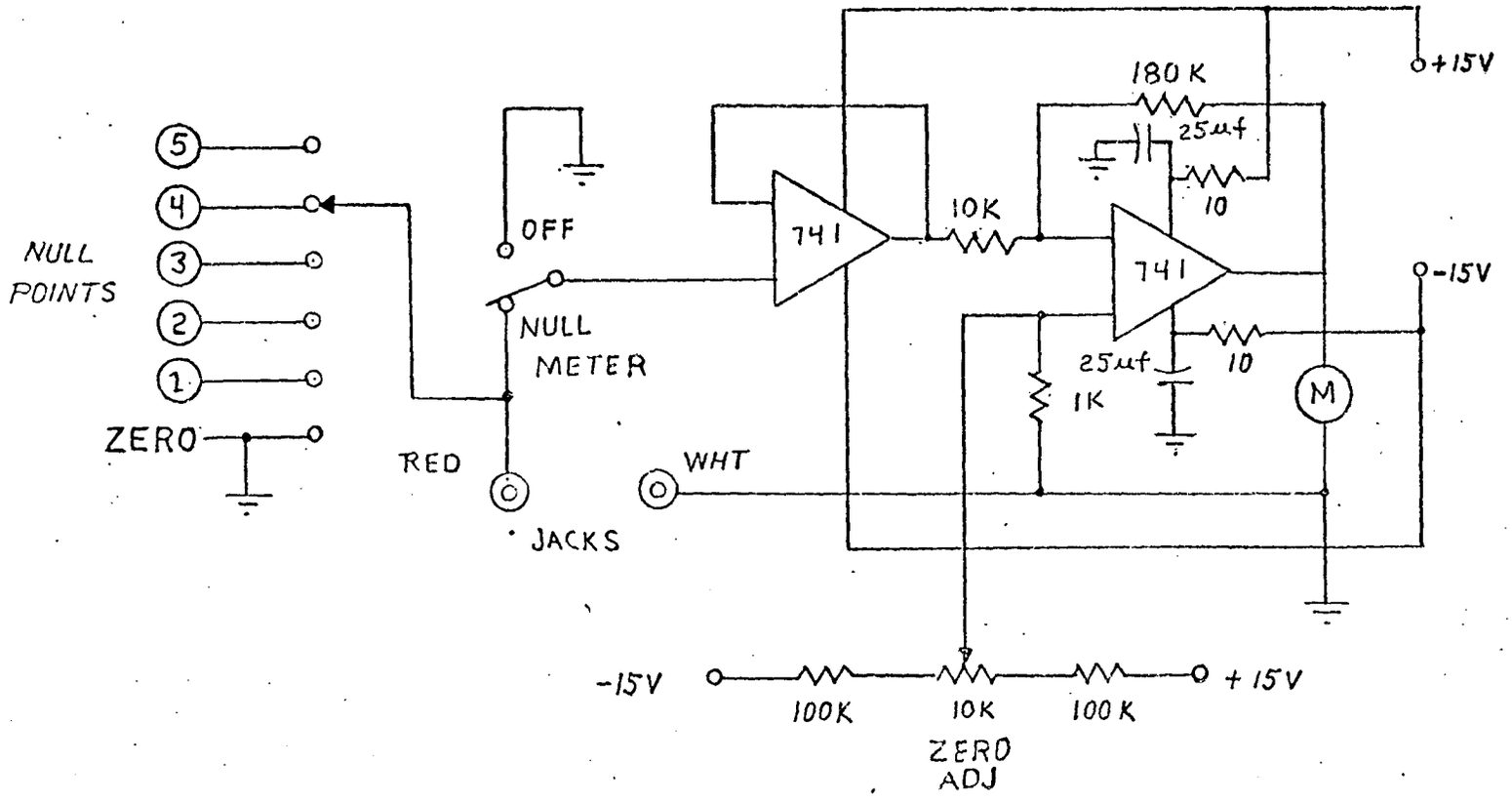

Fig A-2 Null Meter Schematic.

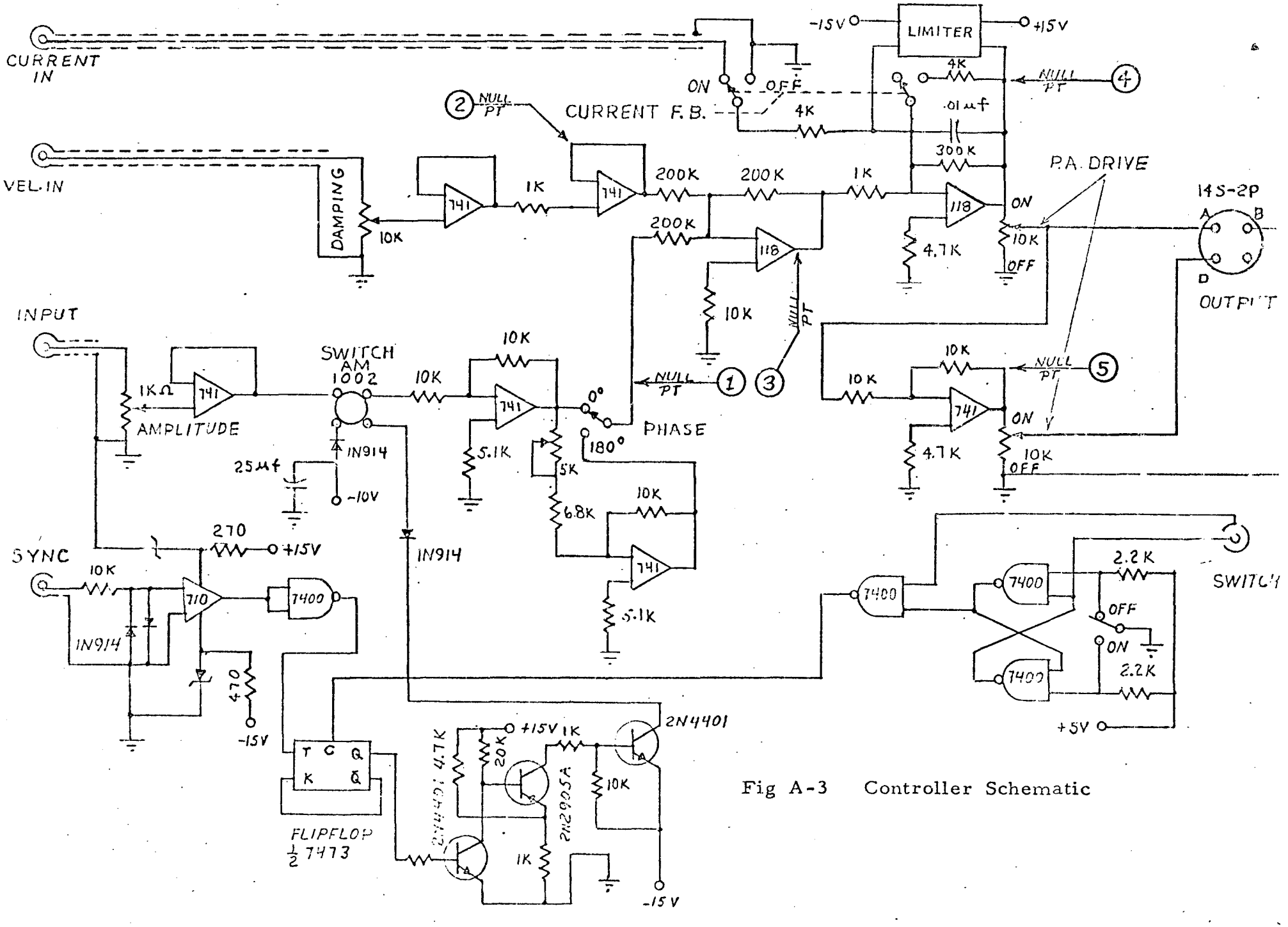

Fig A-3 Controller Schematic

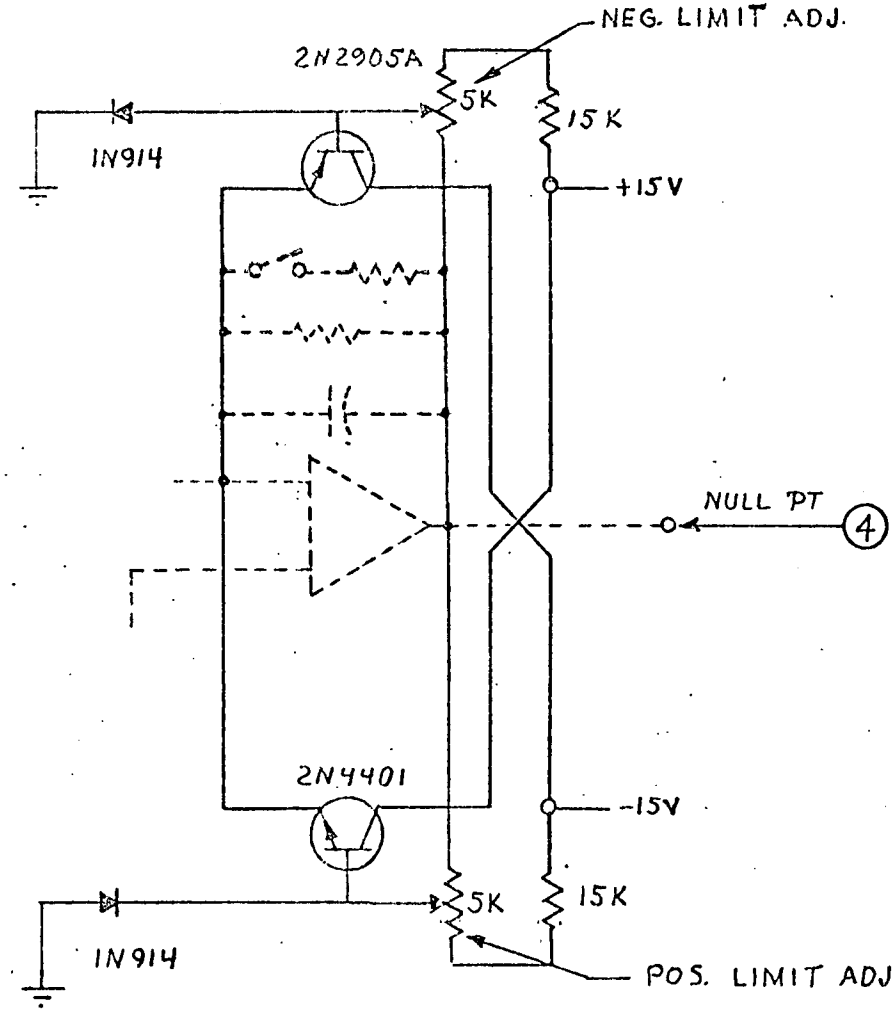

Fig 4 Limiter Schematic

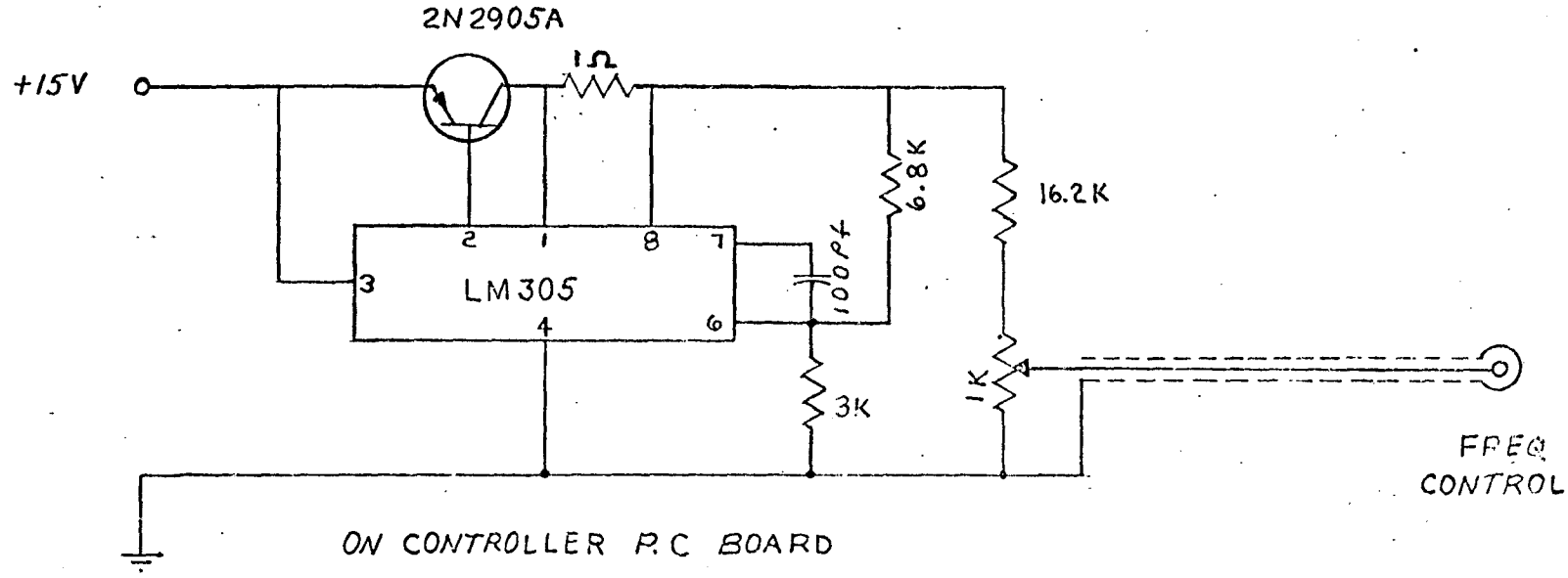

Fig 5 Freqency Control Schematic

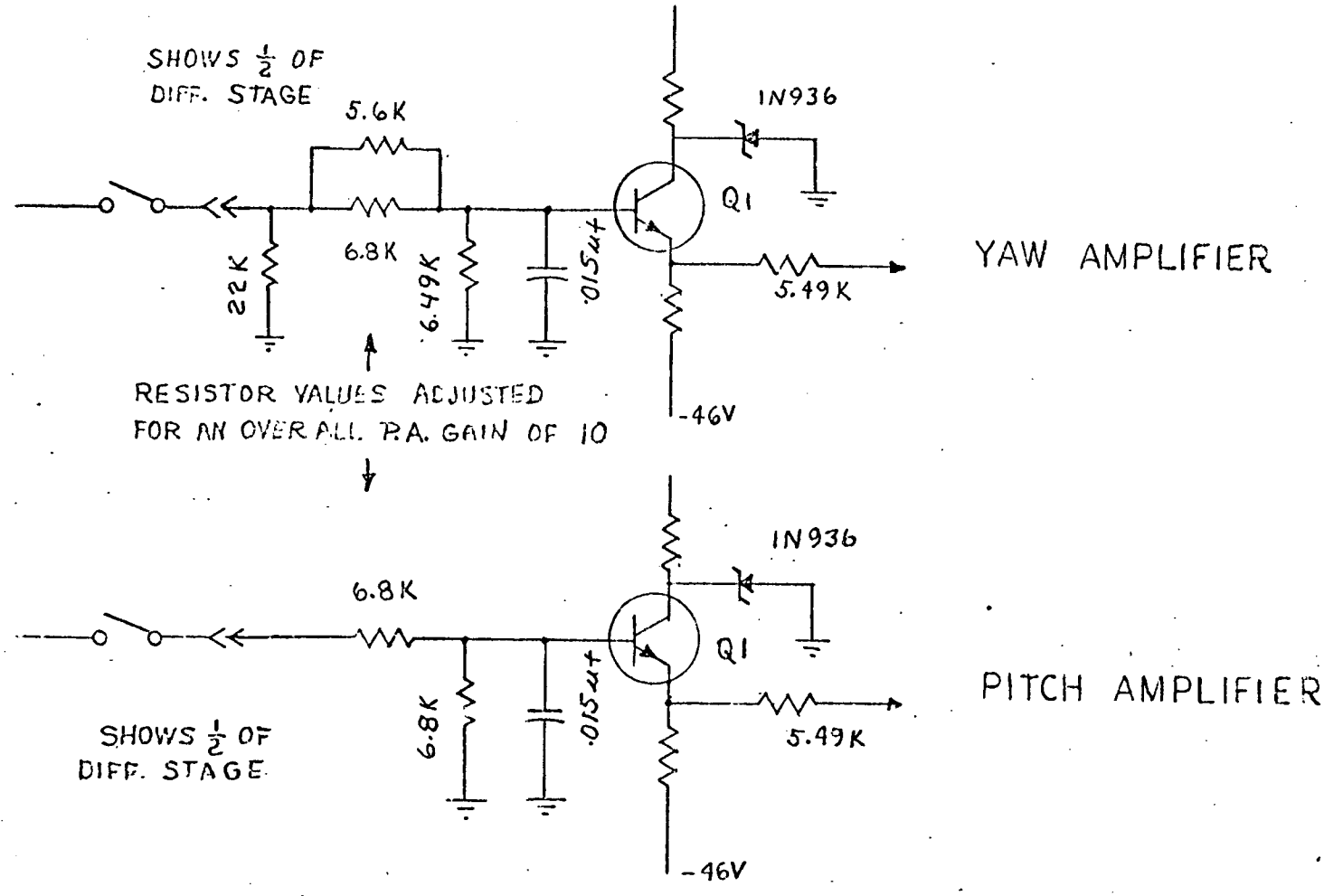

Fig A-6 Input Circuits for Yaw & Pitch Power Amplifiers

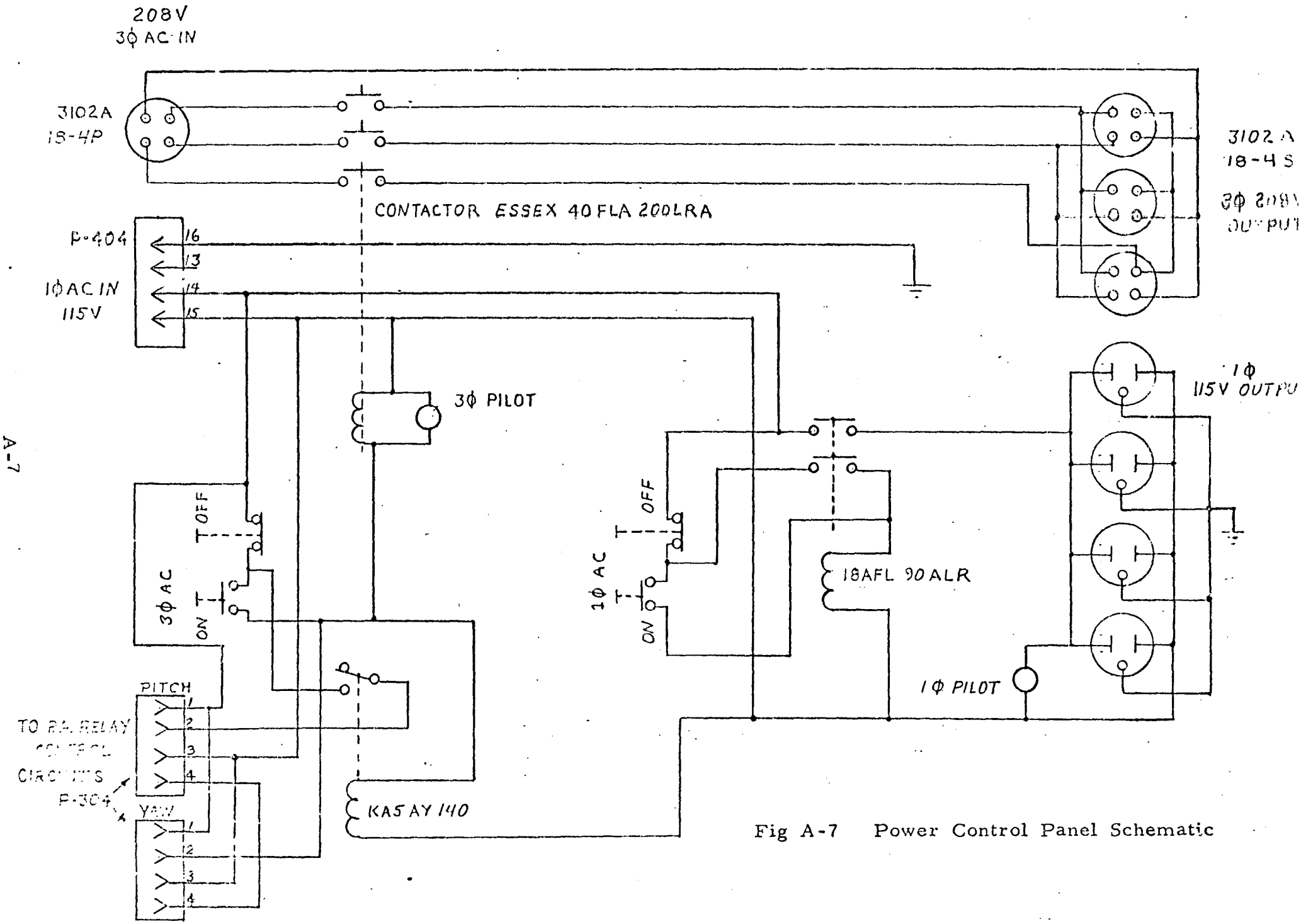

Fig A-7 Power Control Panel Schematic

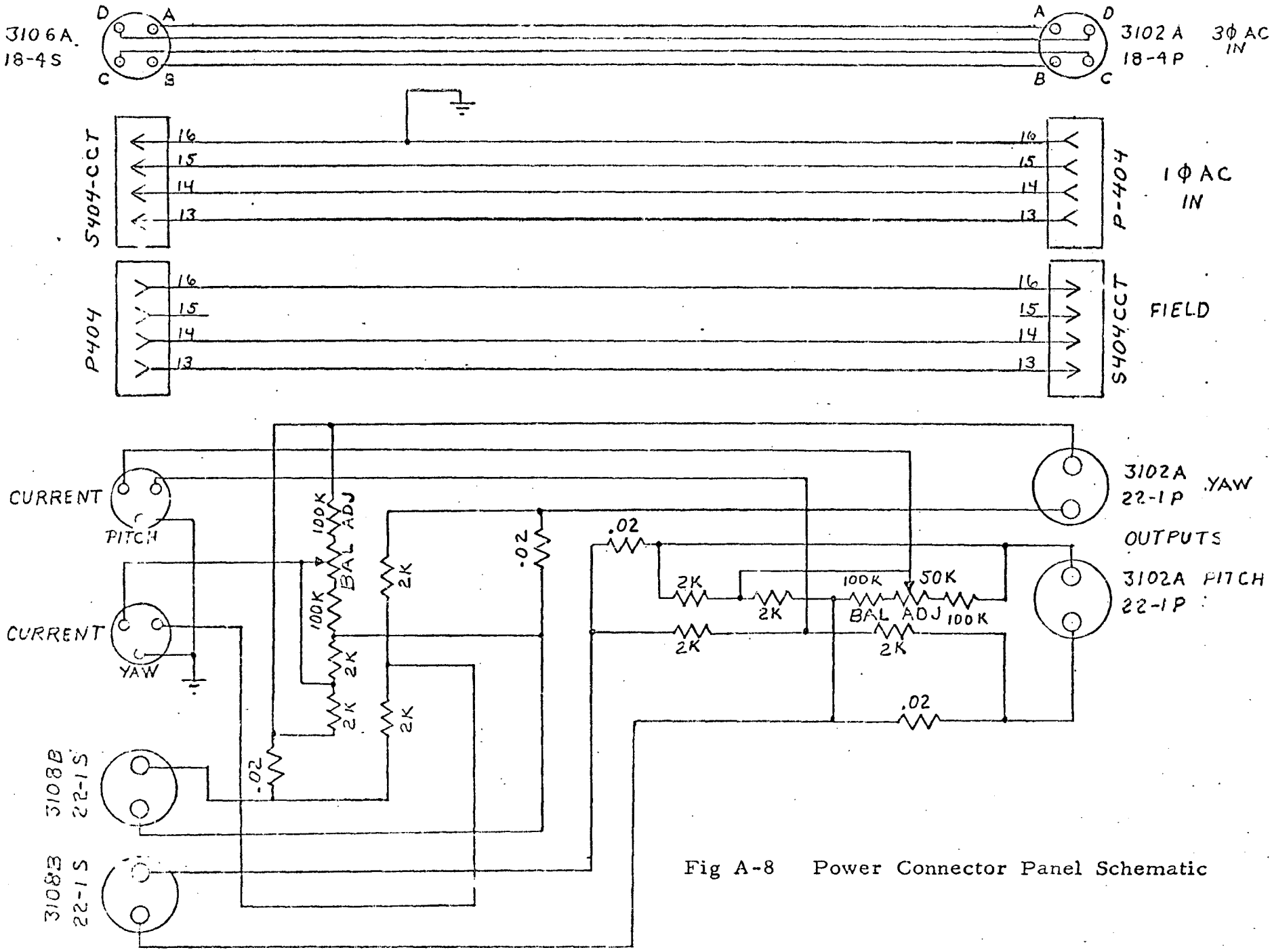

Fig A-8 Power Connector Panel Schematic

APPENDIX B

PATCH PANEL SCHEMATICS

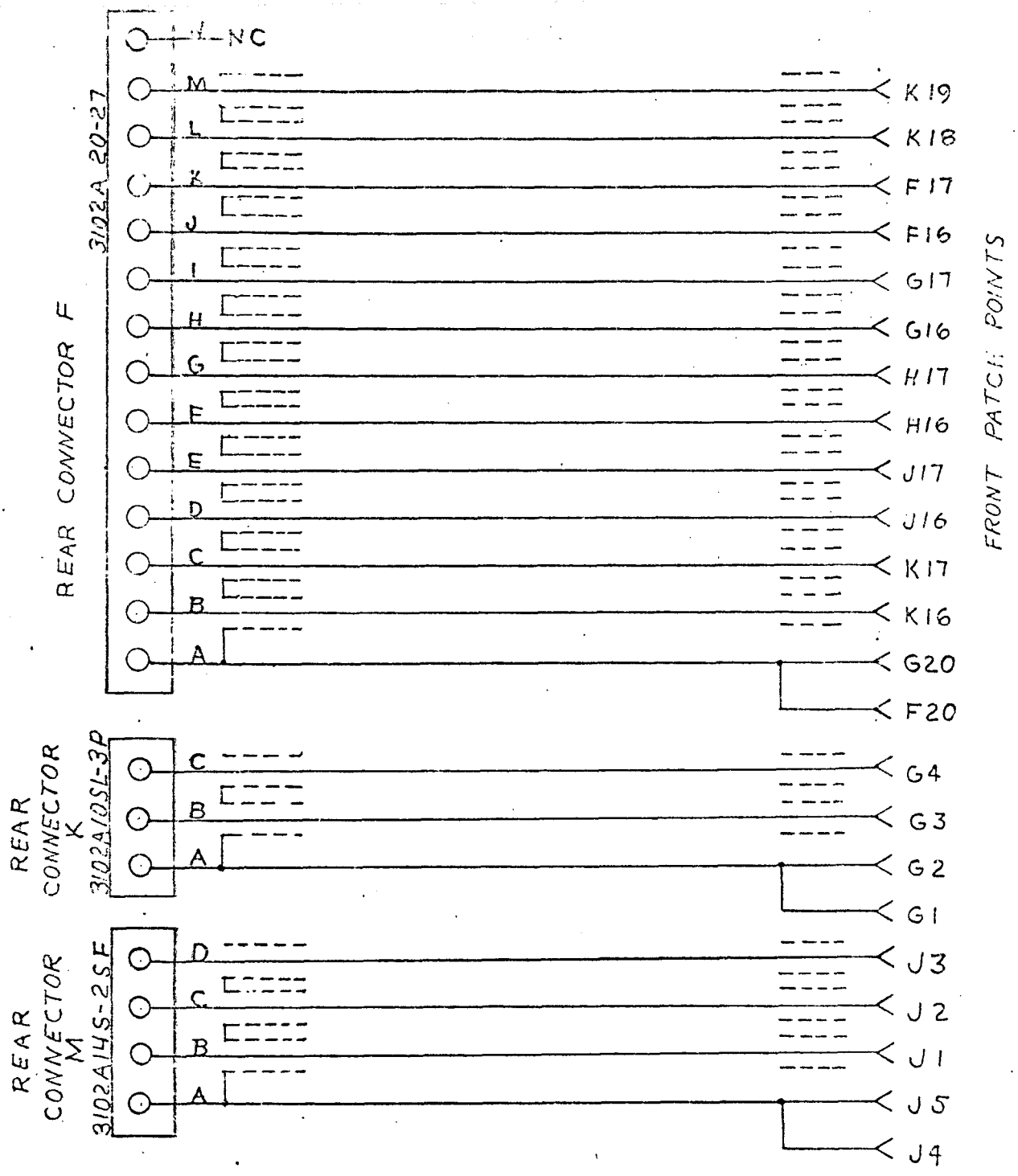

Fig B-1 Connectors F, K, M

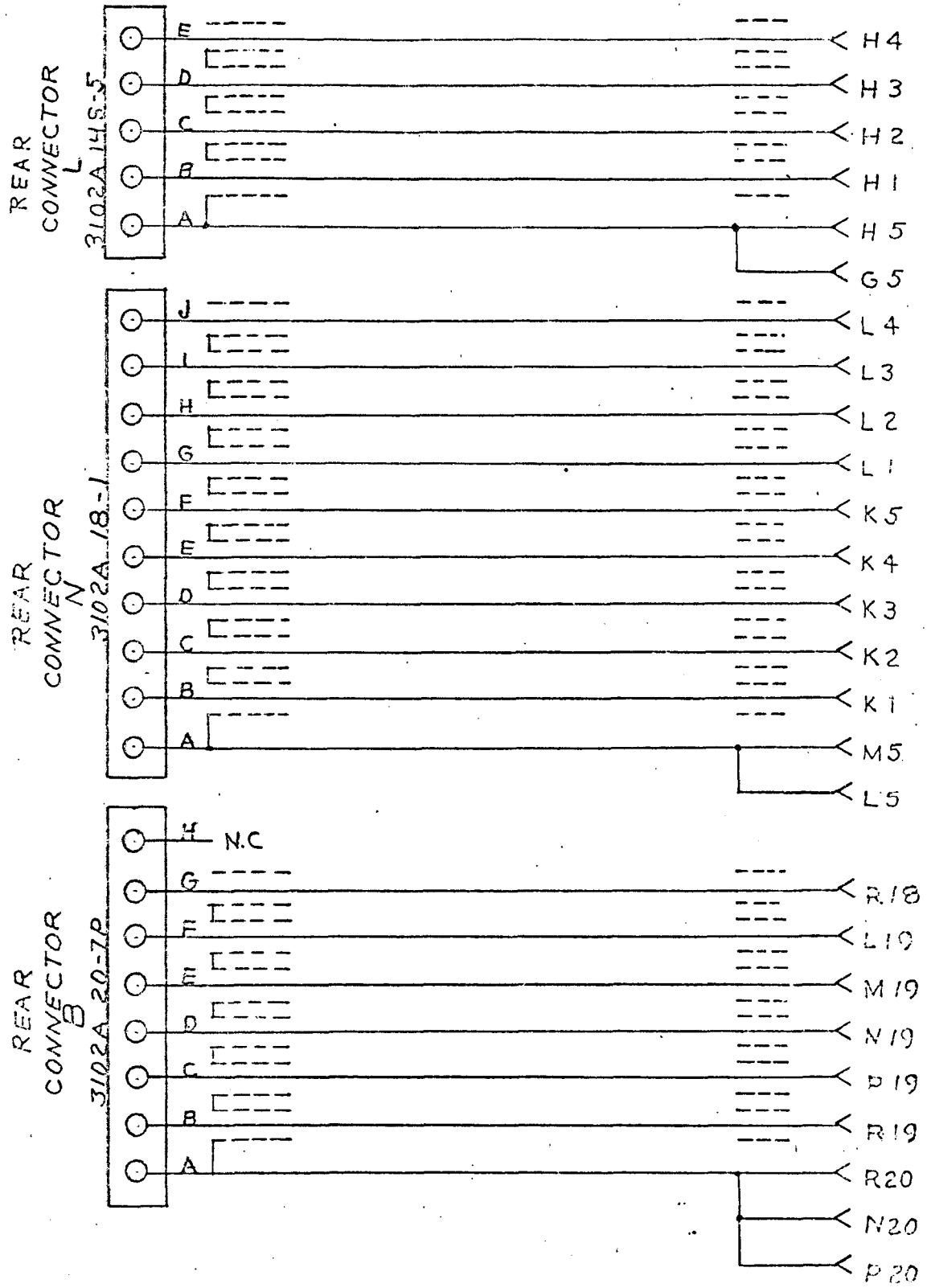

Fig B-2 Connectors L, N, B

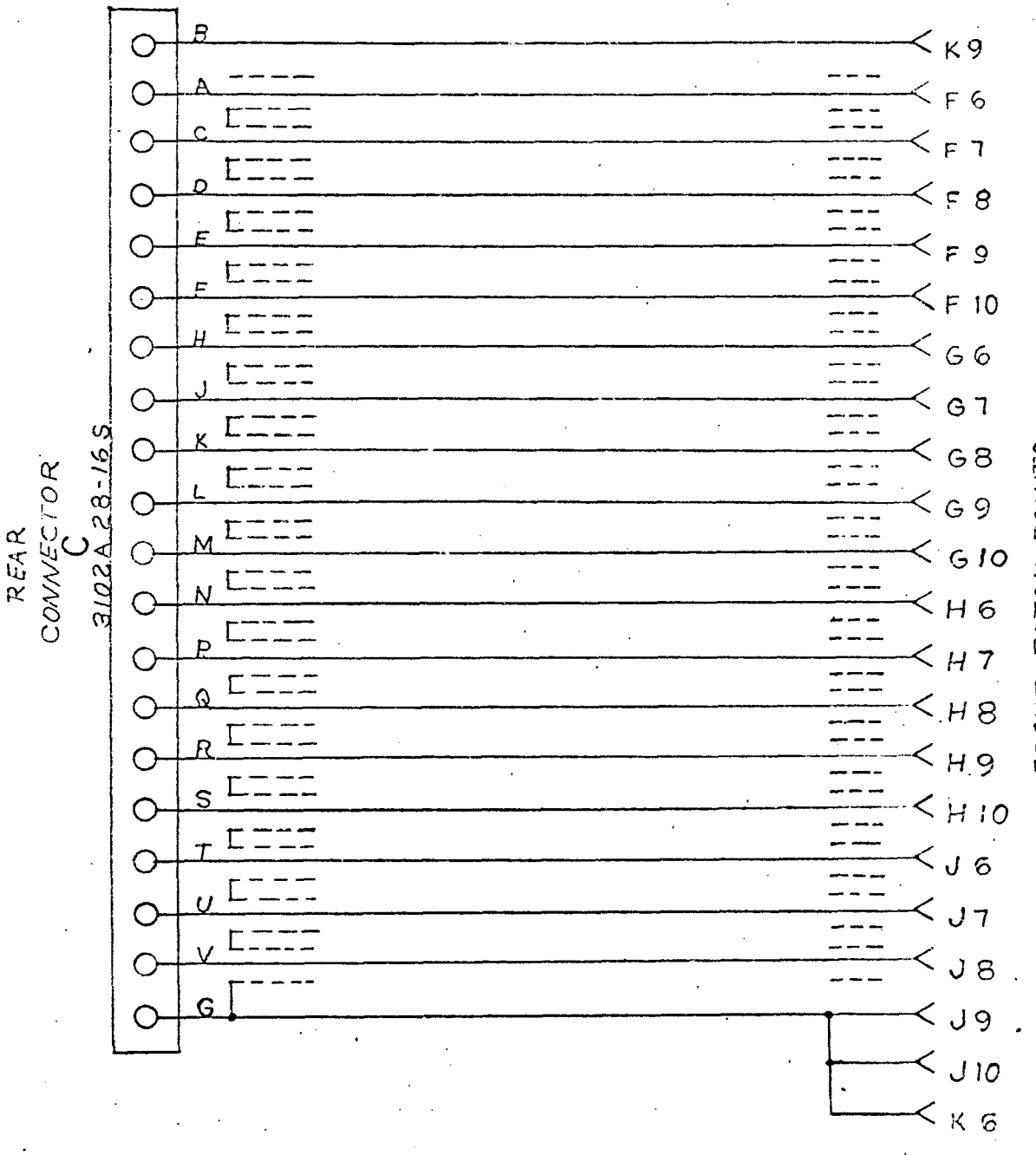

Fig B-3 Connector C

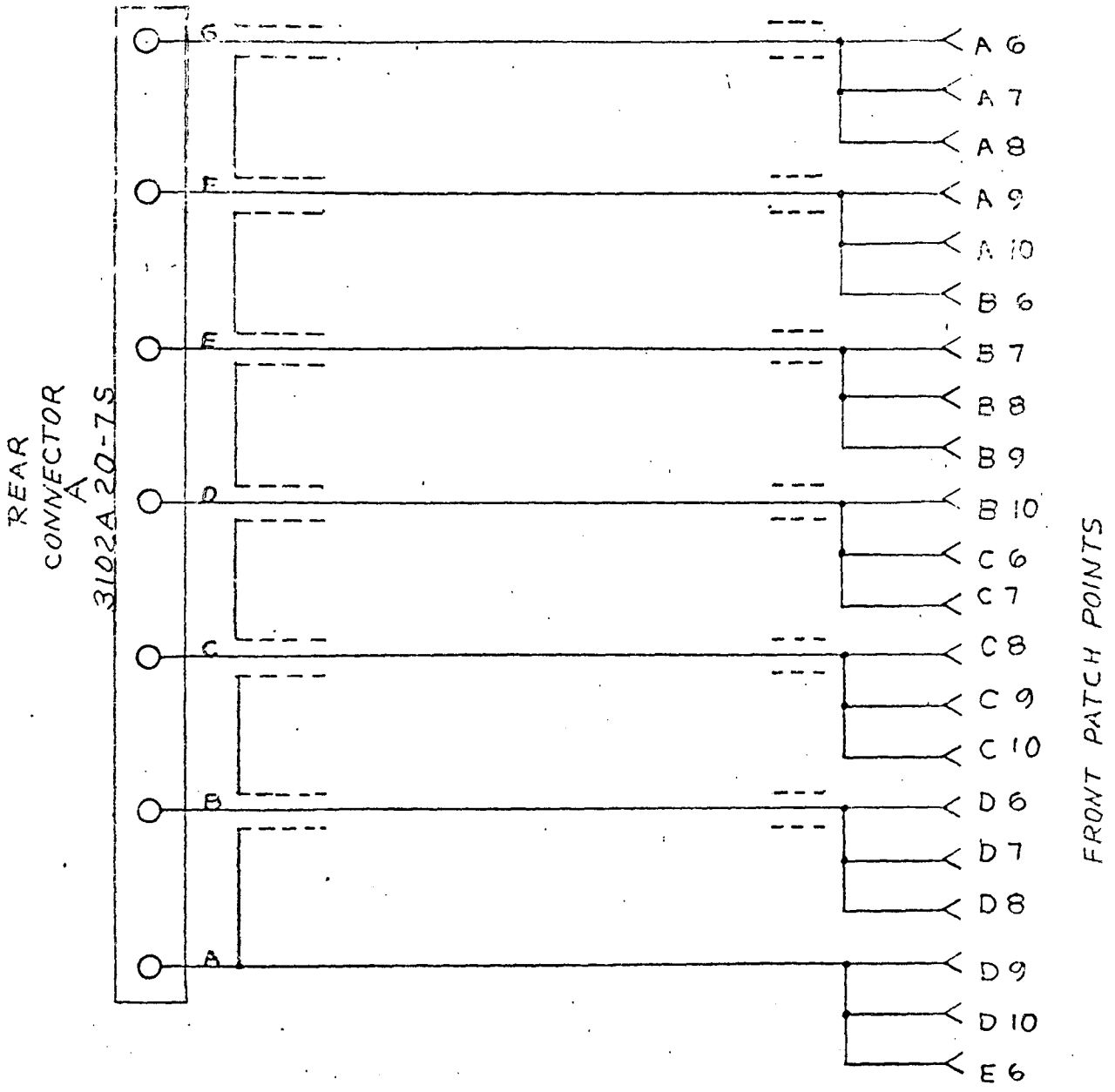

Fig B-4 Connector A

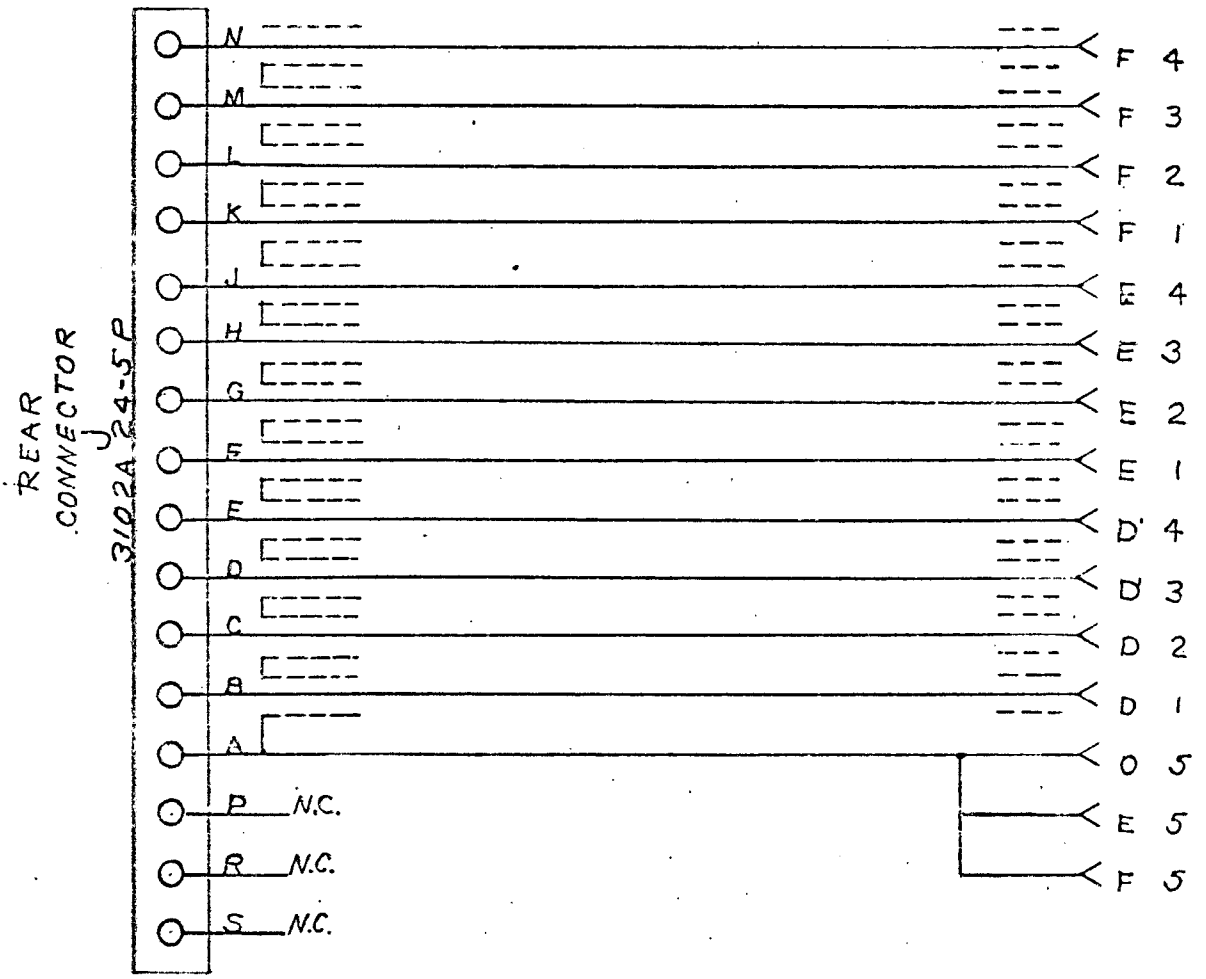

Fig B-5 Connector J

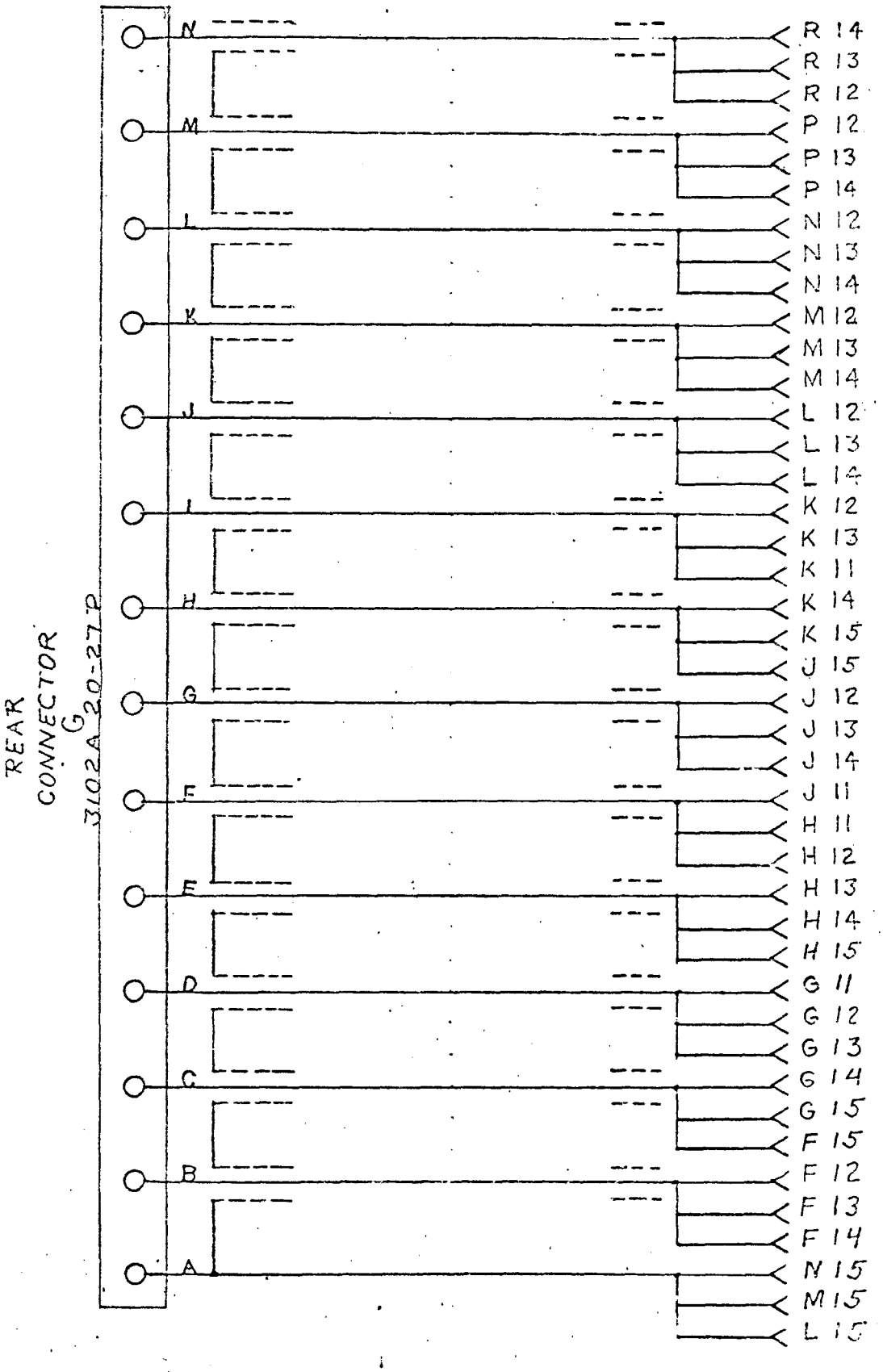

Fig B-6 Connector G

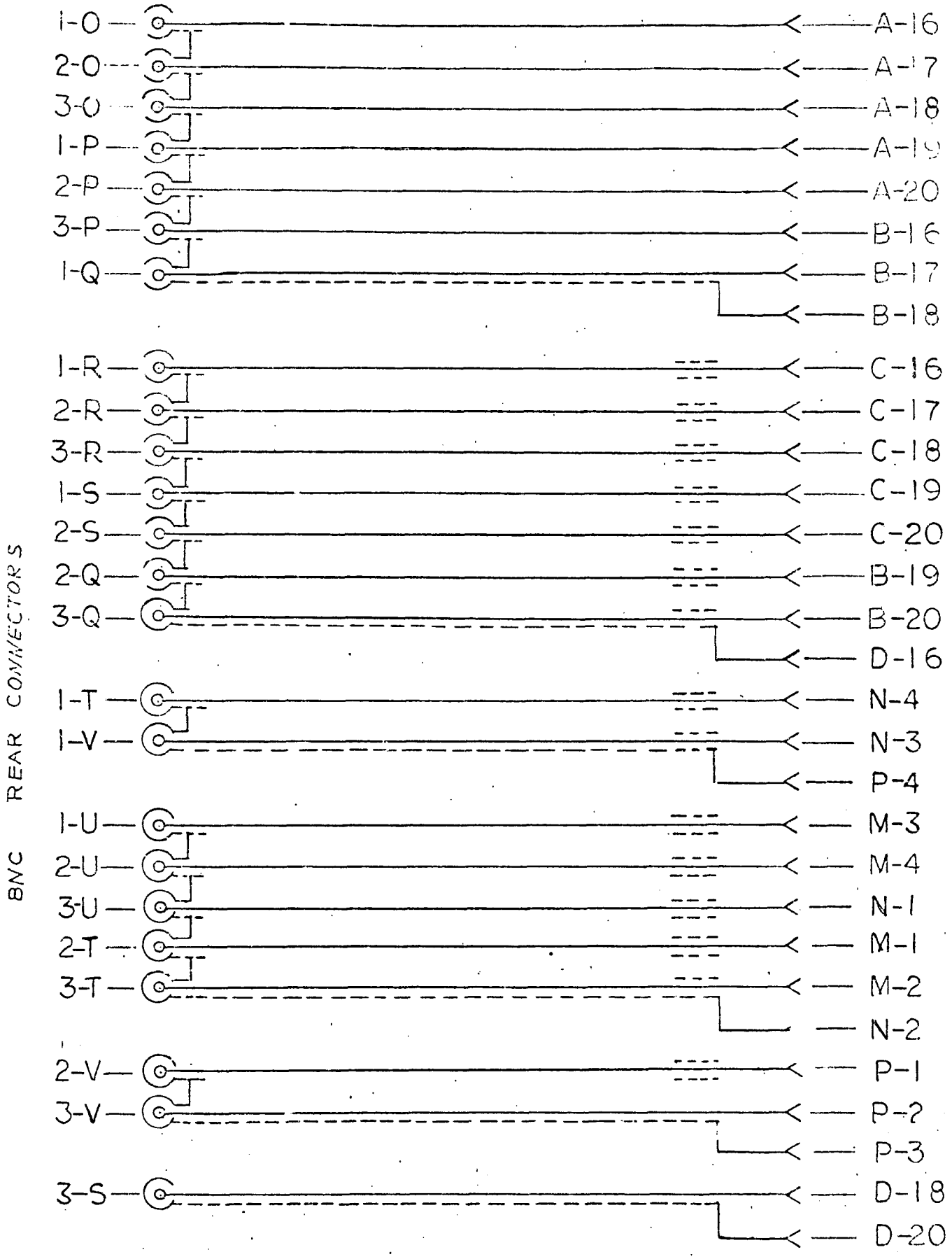

Fig B-7 BNC Connectors

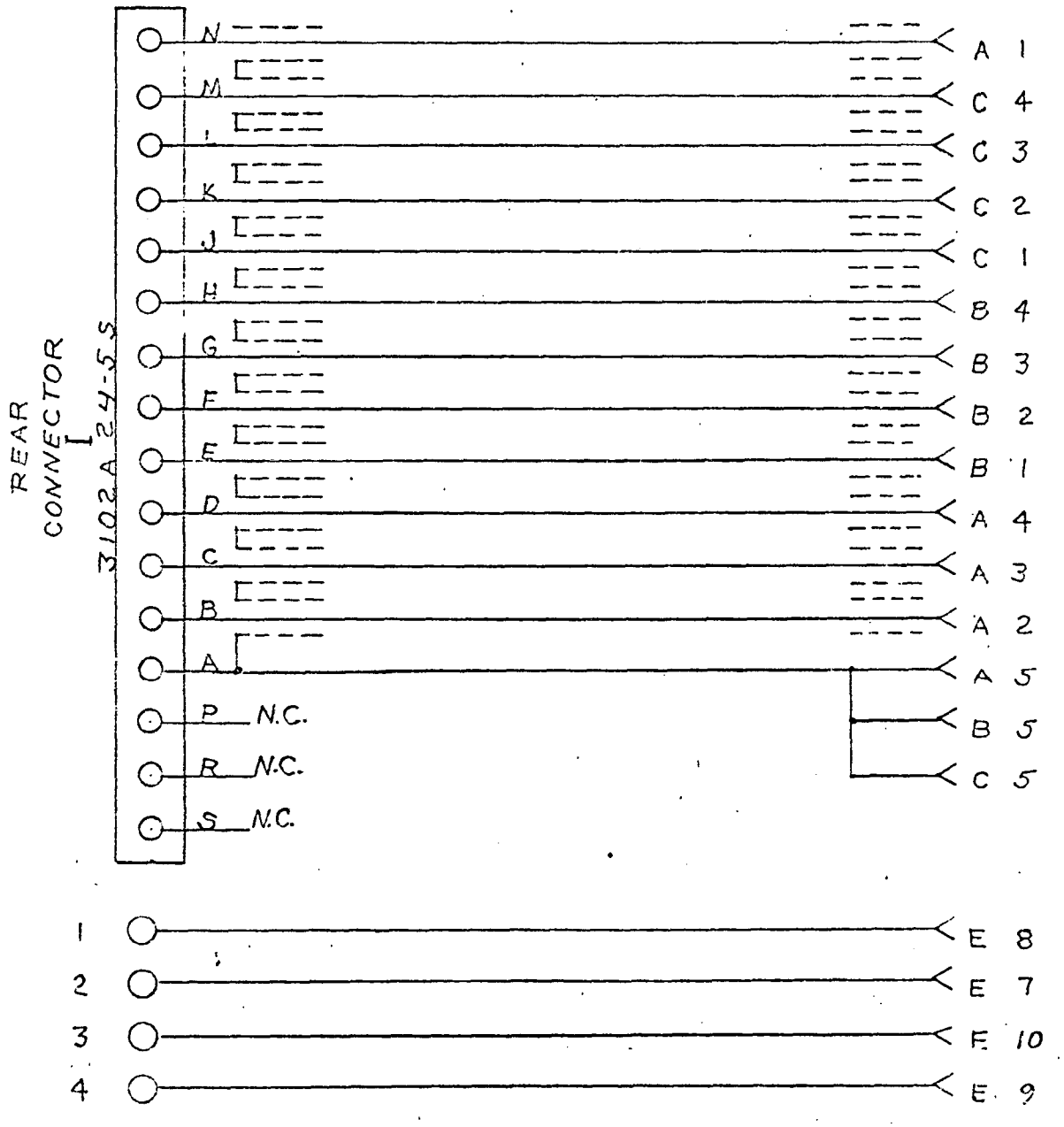

Fig B-8 Connector I

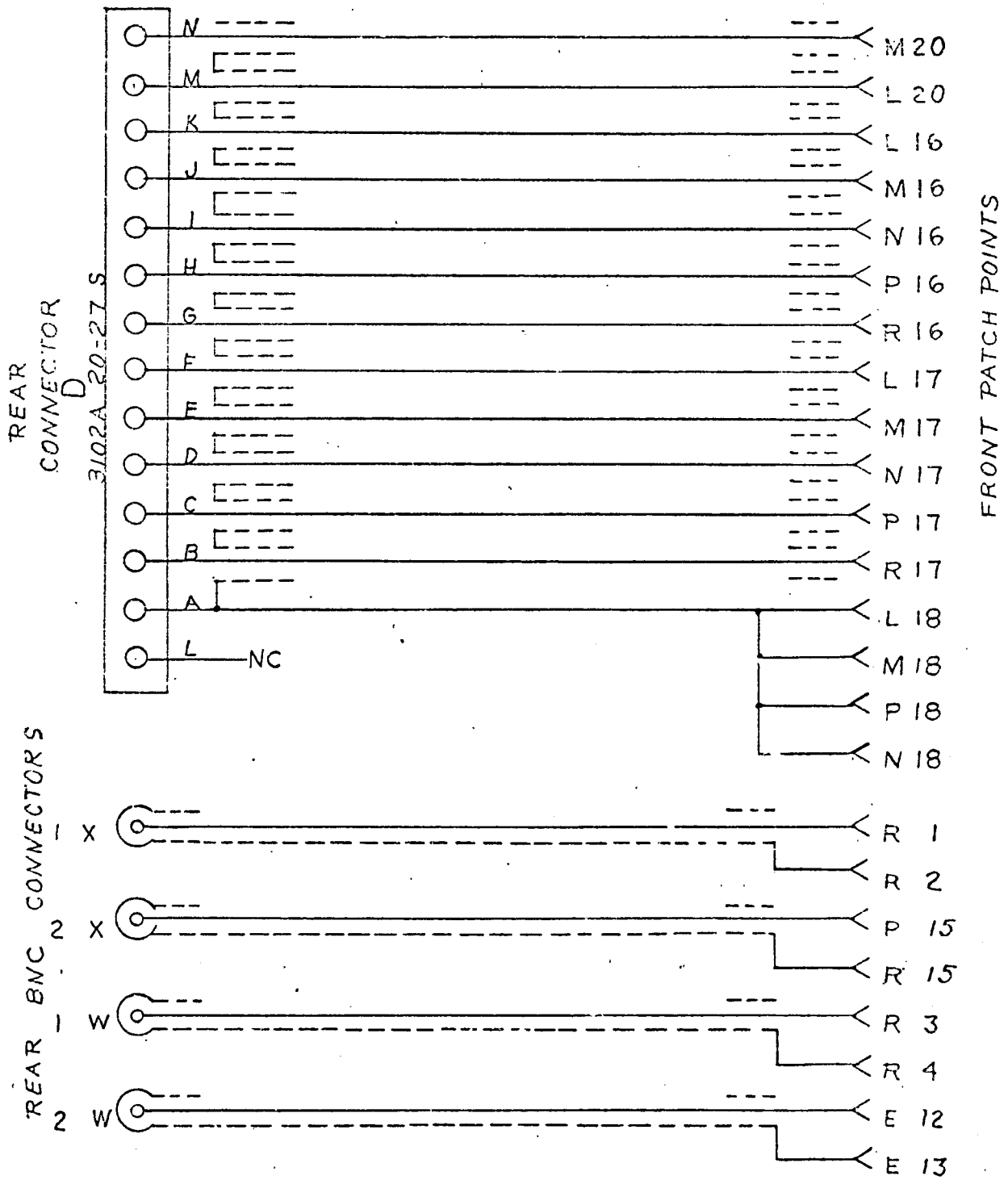

Fig B-9 Connector D and BNC Connectors

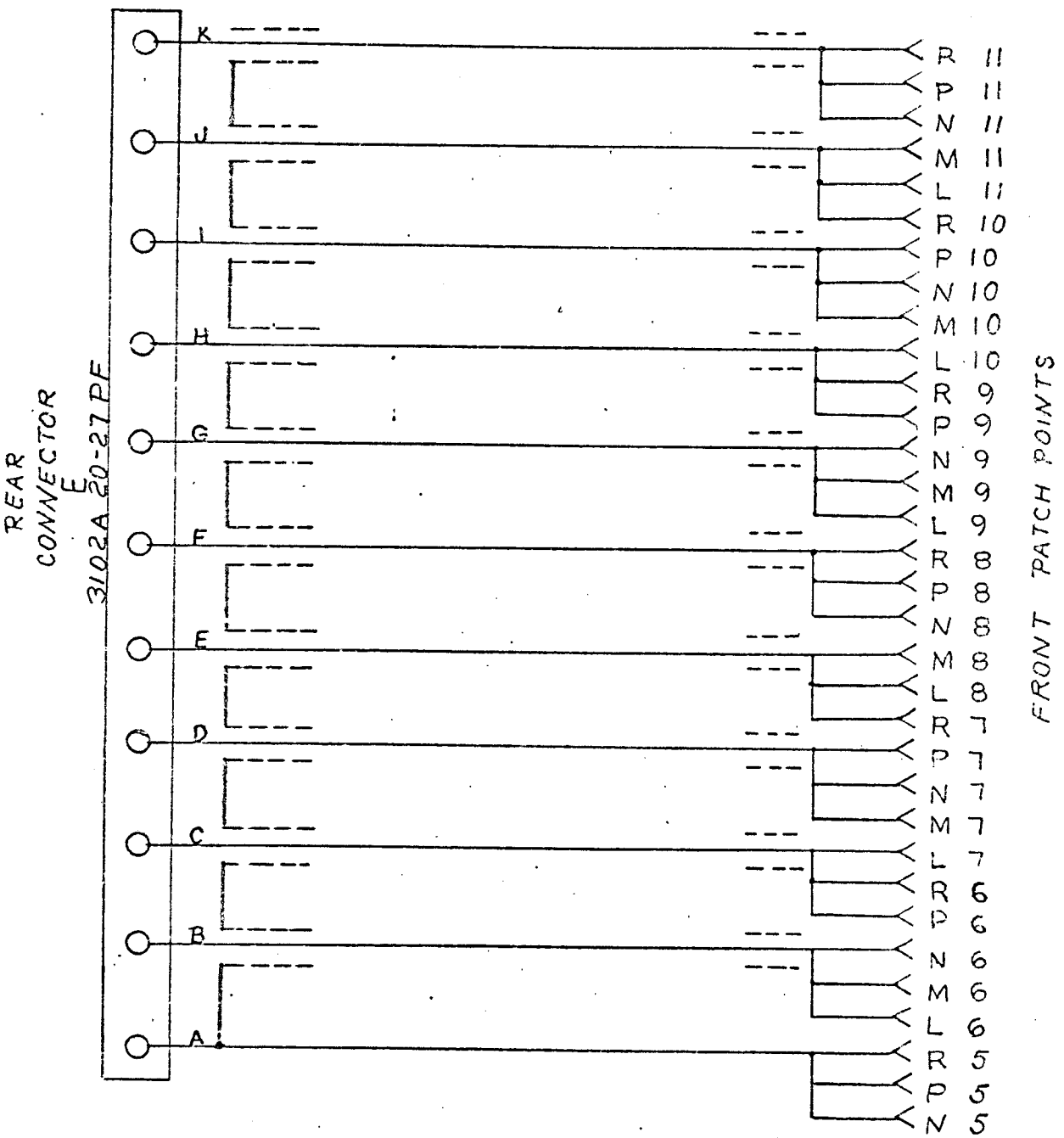

Fig B-10 Connector E

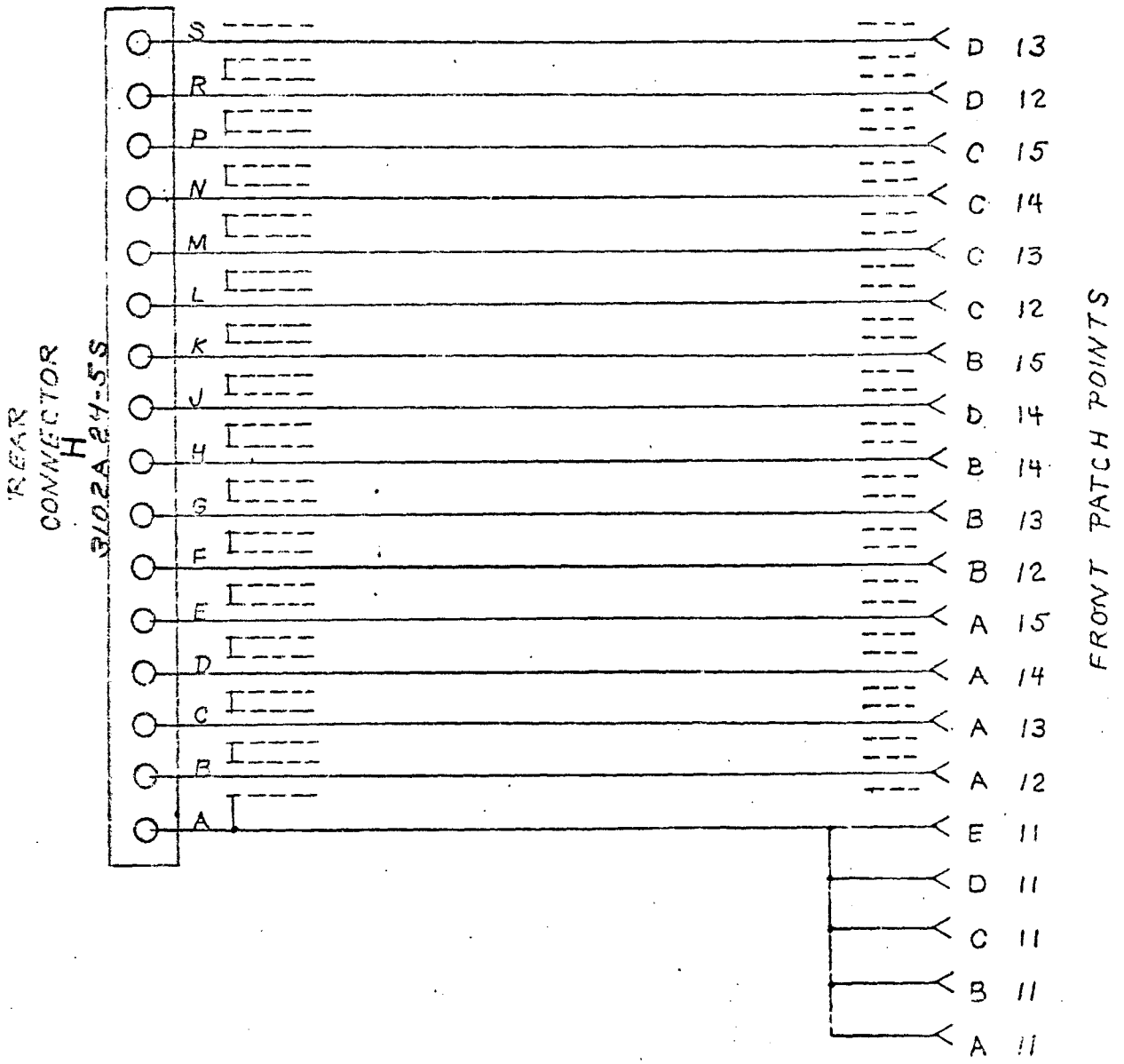

Fig B-11 Connector H